

Theoretical Notes

Note 351

8 February 1984

**PLANE WAVE (EMP) INCIDENCE ON A FINITELY CONDUCTING  
PLANE EARTH WITH THE MAGNETIC FIELD INTENSITY  
PARALLEL TO THE EARTH'S SURFACE\***

H. P. Neff, Jr.  
University of Tennessee  
Knoxville, Tennessee

D. A. Reed  
University of Tennessee  
Knoxville, Tennessee

**Abstract**

The effect of the earth's conductivity and permittivity, along with angle of arrival of the incident plane wave, on the reflected wave are examined. Time-domain results are obtained for both a unit-step incident field and a double-exponential incident field. Results show that for angles less than the Brewster angle it is possible for the composite field to be larger than the incident field.

---

\*The research reported in this Note was performed under Subcontract No. 7685 PA S38 with Union Carbide Corporation.

## I. INTRODUCTION

The phasor form for the plane wave reflected from plane wave incidence on a plane earth is well known [1,2], and is easily derived. The only case considered in this work is that where the magnetic field vector is parallel to the earth's surface. The time-domain form of this reflected wave can be obtained by finding the inverse Fourier transform of the product of the coefficient of reflection and the Fourier transform of the incident wave. An alternate approach is that of convolving the time-domain form of the incident wave with the unit-impulse response (or inverse Fourier transform of the coefficient of reflection). Unfortunately, this impulse response has no closed form, so the former method was chosen. The defining integral for the inverse Fourier transform was converted into a real integral and evaluated numerically using a digital computer.

## II. FORMULATION OF THE PROBLEM

The coefficient of reflection is defined here to be the ratio of the magnitude of the reflected electric field intensity to the magnitude of the incident electric field intensity at the (plane) earth's surface. The phasor form of this reflection coefficient is given by

$$\Gamma_{II}(\omega) = \frac{E_r(\omega)}{E_i(\omega)} = - \frac{1 - \frac{1}{\sqrt{\epsilon_R} \sin \theta} \sqrt{1 - \frac{\sigma/\epsilon}{\sigma/\epsilon + j\omega}} \sqrt{1 - \frac{\cos^2 \theta}{\epsilon_R} (1 - \frac{\sigma/\epsilon}{\sigma/\epsilon + j\omega})}}{1 + \frac{1}{\sqrt{\epsilon_R} \sin \theta} \sqrt{1 - \frac{\sigma/\epsilon}{\sigma/\epsilon + j\omega}} \sqrt{1 - \frac{\cos^2 \theta}{\epsilon_R} (1 - \frac{\sigma/\epsilon}{\sigma/\epsilon + j\omega})}} \quad (1)$$

for Figure 1. It has been assumed that the plane wave approaches the earth in free space ( $\mu_0, \epsilon_0$ ) and the earth has the frequency independent parameters  $\mu_0 = 4\pi \times 10^{-7}$  (free space permeability),  $\epsilon = \epsilon_R \epsilon_0$ ,  $\epsilon_0 = 10^{-9}/36\pi$  (free space permittivity), and  $\sigma$  (conductivity). Notice that codirected tangential components of E are assumed in Figure 1, and a negative sign appears in (1). Thus,  $\Gamma_{II} \rightarrow -1$  for  $\sigma \rightarrow \infty$ .

The following definitions simplify the appearance of equation (1):

$$\alpha_0 \equiv \sigma/\epsilon = \sigma/(\epsilon_0 \epsilon_R), 1/\alpha_0 = \text{relaxation time} \quad (2)$$

$$\beta \equiv \frac{\sqrt{\epsilon_R - \cos^2 \theta}}{\epsilon_R \sin \theta} \quad (3)$$

$$\gamma \equiv \frac{\sigma/\epsilon_0}{\epsilon_R - \cos^2 \theta} \quad (4)$$

$$\Gamma_{II} = - \frac{\alpha_0 + j\omega - \beta \sqrt{-\omega^2 + j\omega \gamma}}{\alpha_0 + j\omega + \beta \sqrt{-\omega^2 + j\omega \gamma}} \quad (5)$$

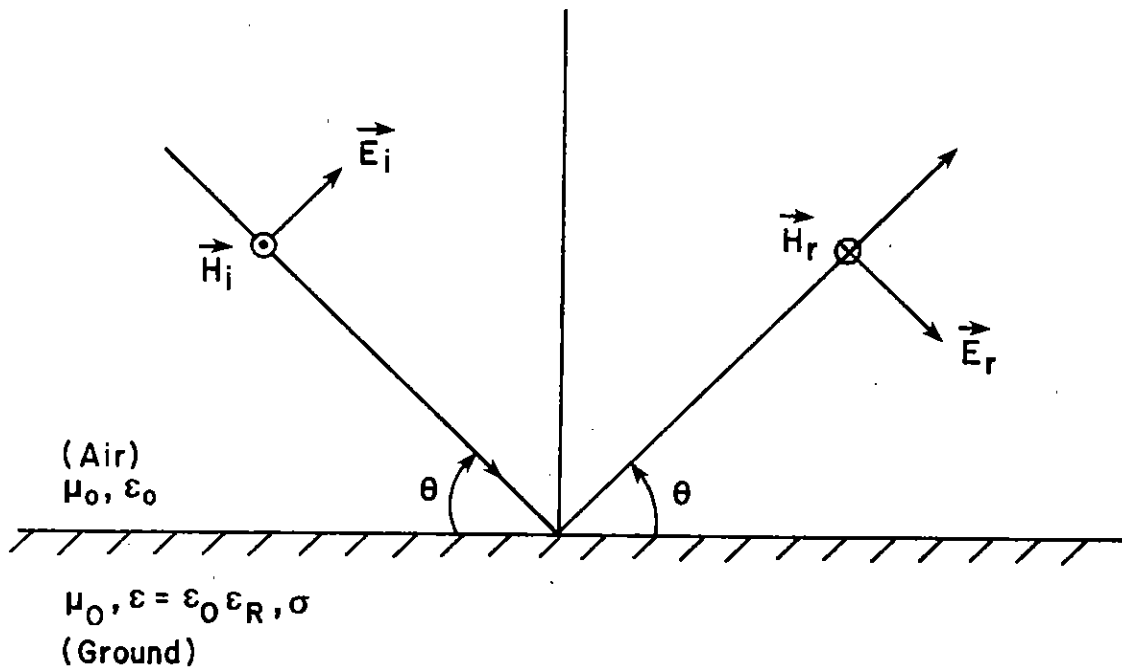


Figure 1. Geometry of the problem: plane wave incidence on a plane earth with the magnetic field parallel to the earth's surface.

The special case  $\sigma = 0$  and (therefore)  $\alpha_n = \gamma = 0$  is considered first. For this case equation (5) becomes

$$\Gamma_{II} = \frac{\beta - 1}{\beta + 1} \quad (\sigma = 0) \quad (6)$$

and there will be no reflection ( $\Gamma_{II} = 0$ ) when  $\beta = 1$ . The angle  $\theta_B$  for this condition is called the Brewster angle or polarizing angle. It is calculated from equation (3) with  $\beta = 1$ :

$$\theta_B = \cos^{-1} \sqrt{\frac{\epsilon_R}{\epsilon_R + 1}} \quad (\text{Brewster angle}) \quad (7)$$

Although there is no true Brewster angle for the general case ( $\sigma > 0, \epsilon_R > 1$ ), it is informative to consider the high frequency behavior of  $\Gamma_{II}$  for  $\beta < 1$ ,  $\beta = 1$ , and  $\beta > 1$ . The behavior of  $\Gamma_{II}(\omega)$  for high frequency determines the early time behavior of  $T_{II}(t)$ .

Case I  $\beta < 1, \theta > \theta_B$

$$\Gamma_{II}(\omega) \rightarrow \frac{1 - \beta}{1 + \beta} \underline{180^\circ} = \frac{\beta - 1}{\beta + 1}$$

$$\omega \rightarrow \infty$$

Case II  $\beta = 1, \theta = \theta_B$

$$\Gamma_{II}(\omega) \rightarrow \frac{(\epsilon_R - 1)\alpha_n}{4\omega\epsilon_R} \underline{90^\circ}$$

$$\omega \rightarrow \infty$$

Case III  $\beta > 1, \theta < \theta_B$

$$\Gamma_{II}(\omega) \rightarrow \frac{\beta - 1}{\beta + 1} = \underline{0^\circ} = \frac{\beta - 1}{\beta + 1}$$

$$\omega \rightarrow \infty$$

This behavior is exhibited in Figure 2 and Figure 3 where the magnitude and angle (respectively) are shown as functions of normalized frequency,  $\omega/a_0$ , for  $\epsilon_R = 10$  and  $\theta_B = 17.55^\circ$ . The case  $\theta < \theta_B$  is distinctly different.

Based on the results of the preceding paragraph, it seems quite likely that the ground reflected wave from an e.m.p. may add to the incident wave for early time and  $\theta < \theta_B$ . This, along with the general behavior of the reflected wave, is examined by calculating

$$E_r(t) = F^{-1}\{E_r(\omega)\} = F^{-1}\{E_i(\omega)\Gamma_{II}(\omega)\} \quad (8)$$

for  $\sigma = 0.01, 0.001$ ;  $\epsilon_R = 10, 15$ ;  $\theta = 10^\circ, 14.48^\circ (= \theta_B \text{ for } \epsilon_R = 15), 17.55^\circ (= \theta_B \text{ for } \epsilon_R = 10), 18^\circ, 36^\circ, 54^\circ, 90^\circ$ . The inverse Fourier transform integral was converted into a real integral and evaluated numerically.

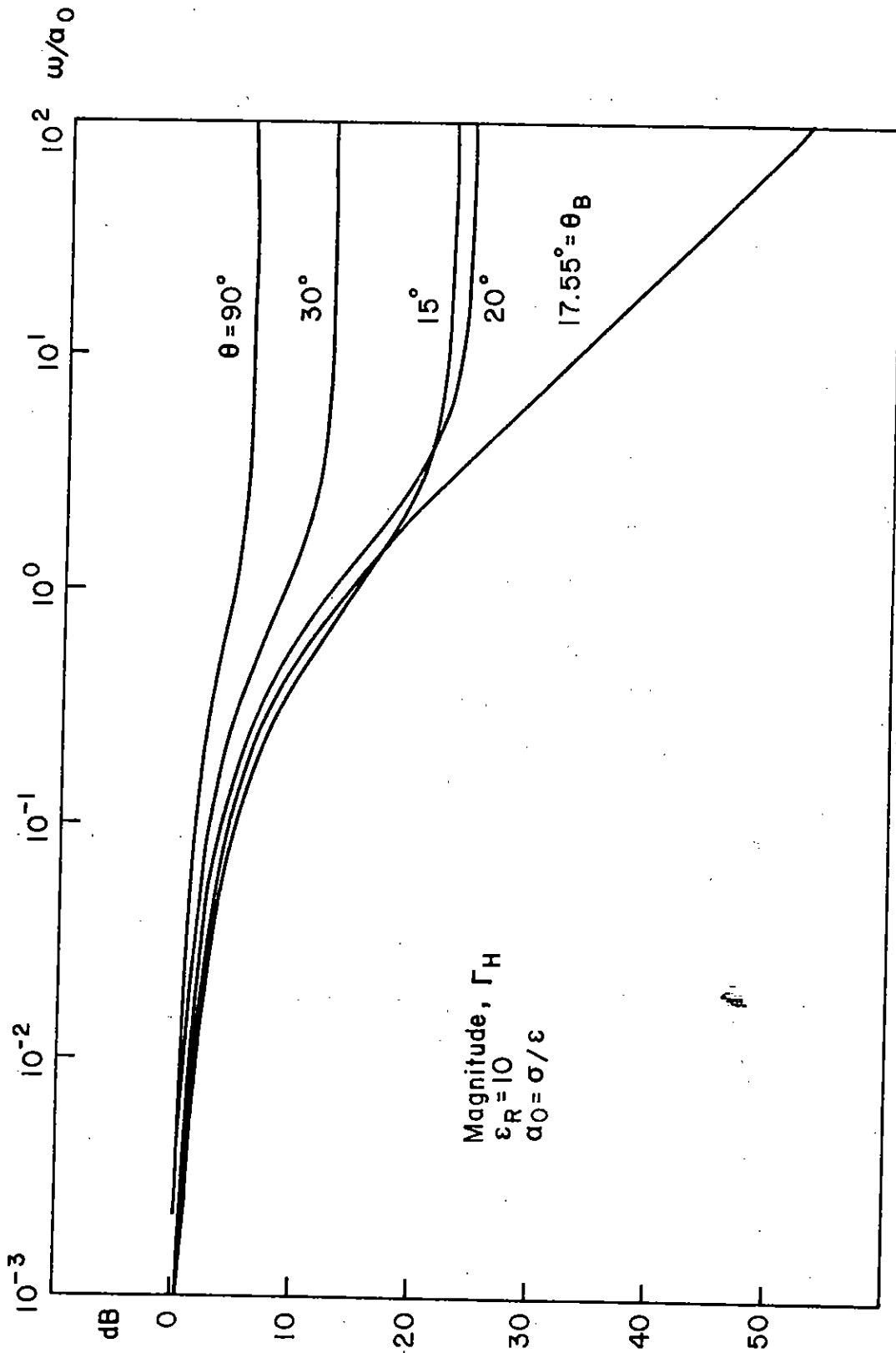


Figure 2.  $|\Gamma_H|$  versus  $\omega/\alpha_0$  with  $\epsilon_R = 10$  for several values of  $\theta$ .

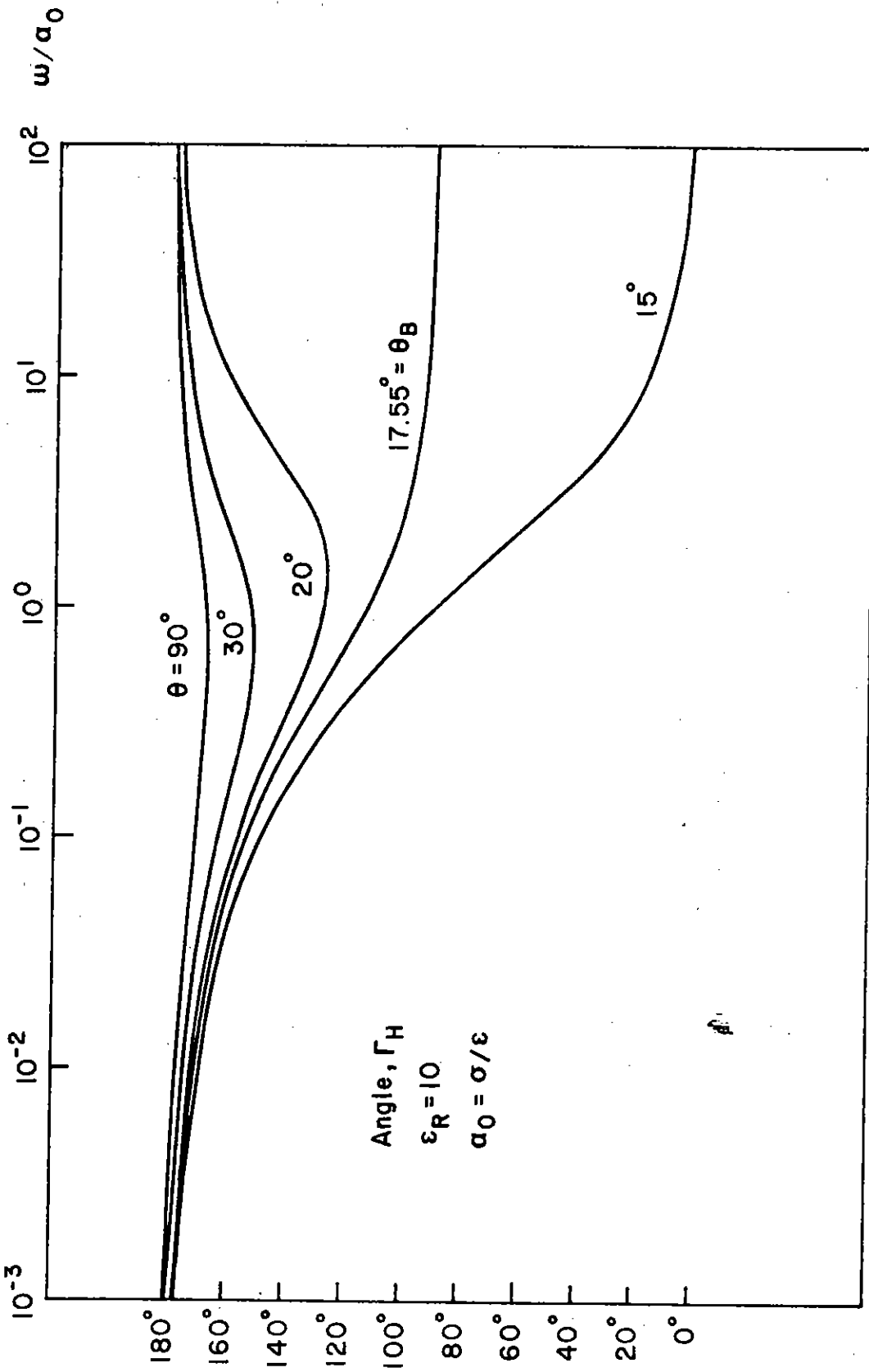


Figure 3.  $\Gamma_H$  versus  $\omega/\alpha_0$  with  $\epsilon_R = 10$  for several values of  $\theta$ .



This behavior is exhibited in Figure 2 and Figure 3 where the magnitude and angle (respectively) are shown as functions of normalized frequency,  $\omega/a_0$ , for  $\epsilon_R = 10$  and  $\theta_B = 17.55^\circ$ . The case  $0 < \theta_B$  is distinctly different.

Based on the results of the preceding paragraph, it seems quite likely that the ground reflected wave from an e.m.p. may add to the incident wave for early time and  $0 < \theta_B$ . This, along with the general behavior of the reflected wave, is examined by calculating

$$E_r(t) = F^{-1}\{E_r(\omega)\} = F^{-1}\{E_i(\omega)R_H(\omega)\} \quad (8)$$

for  $\sigma = 0.01, 0.001$ ;  $\epsilon_R = 10, 15$ ;  $\theta = 10^\circ, 14.48^\circ (= \theta_B \text{ for } \epsilon_R = 15), 17.55^\circ (= \theta_B \text{ for } \epsilon_R = 10), 18^\circ, 36^\circ, 54^\circ, 90^\circ$ . The inverse Fourier transform integral was converted into a real integral and evaluated numerically.

### III. RESULTS

Results are shown in Figures 4 through 17. Notice carefully that  $E_i(t)$  is plotted for comparison purposes, and  $-E_r(t)$  (that is, the negative of the reflected wave) is shown. The incident field at the earth's surface was mathematically modeled by the usual double-exponential form:

$$E_i(t) = E_0 |e^{-\alpha_1 t} - e^{-\alpha_2 t}| \quad (9)$$

$$E_0 = 52,500 \text{ V/m}$$

$$\alpha_1 = 4 \times 10^6 \text{ sec}^{-1}$$

$$\alpha_2 = 478 \times 10^6 \text{ sec}^{-1}$$

or

$$E_i(\omega) = E_0 \left| \frac{1}{\alpha_1 + j\omega} - \frac{1}{\alpha_2 + j\omega} \right| \quad (10)$$

For very low frequencies equation (5) gives  $\Gamma_H \approx -1$ , and therefore the late time behavior of the reflected wave is such that  $E_r(t) \approx -E_i(t)$ . In other words,  $-E_r(t)$  and  $E_i(t)$  should become identical for large  $t$  in Figures 4 through 17. This is the case.

For  $0 < \theta_B$ , it is possible, as suspected, for the reflected wave to add to the incident wave. In order to demonstrate this explicitly, the composite wave is shown in Figures 18, 19, 20. The composite wave results from adding the incident wave and the time-delayed reflected wave. The time delay is given by  $2h \sin \theta/c$ , where  $c = 1/\sqrt{\mu_0 \epsilon_0}$  is the speed of light, and  $h$ , the height above ground, was chosen to be 10 meters (typical of power transmission lines). It is

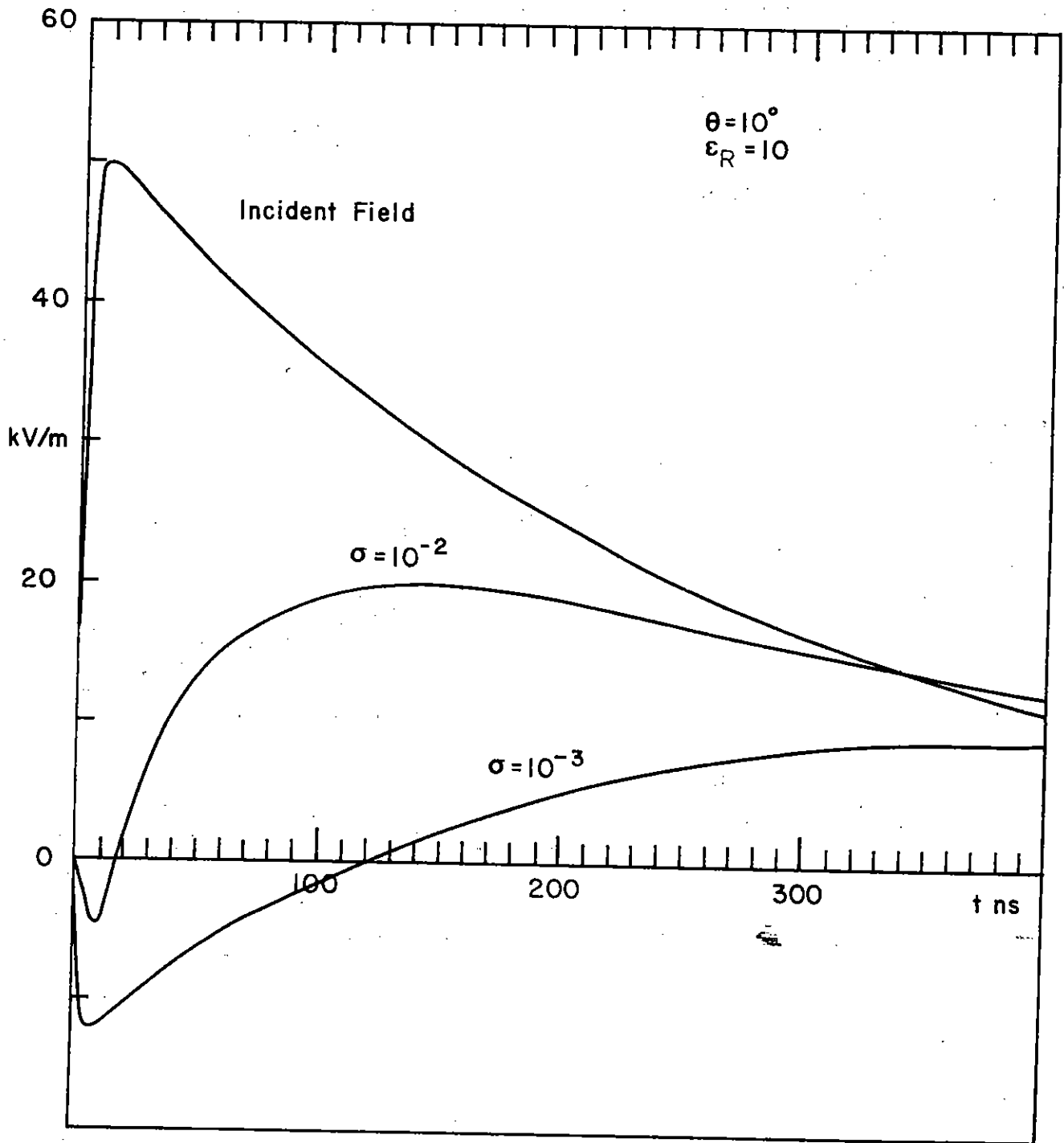


Figure 4. Reflected electric field (-):  $\epsilon_R = 10$ ,  $\theta = 10^\circ$ . The incident field is given by equation 10.

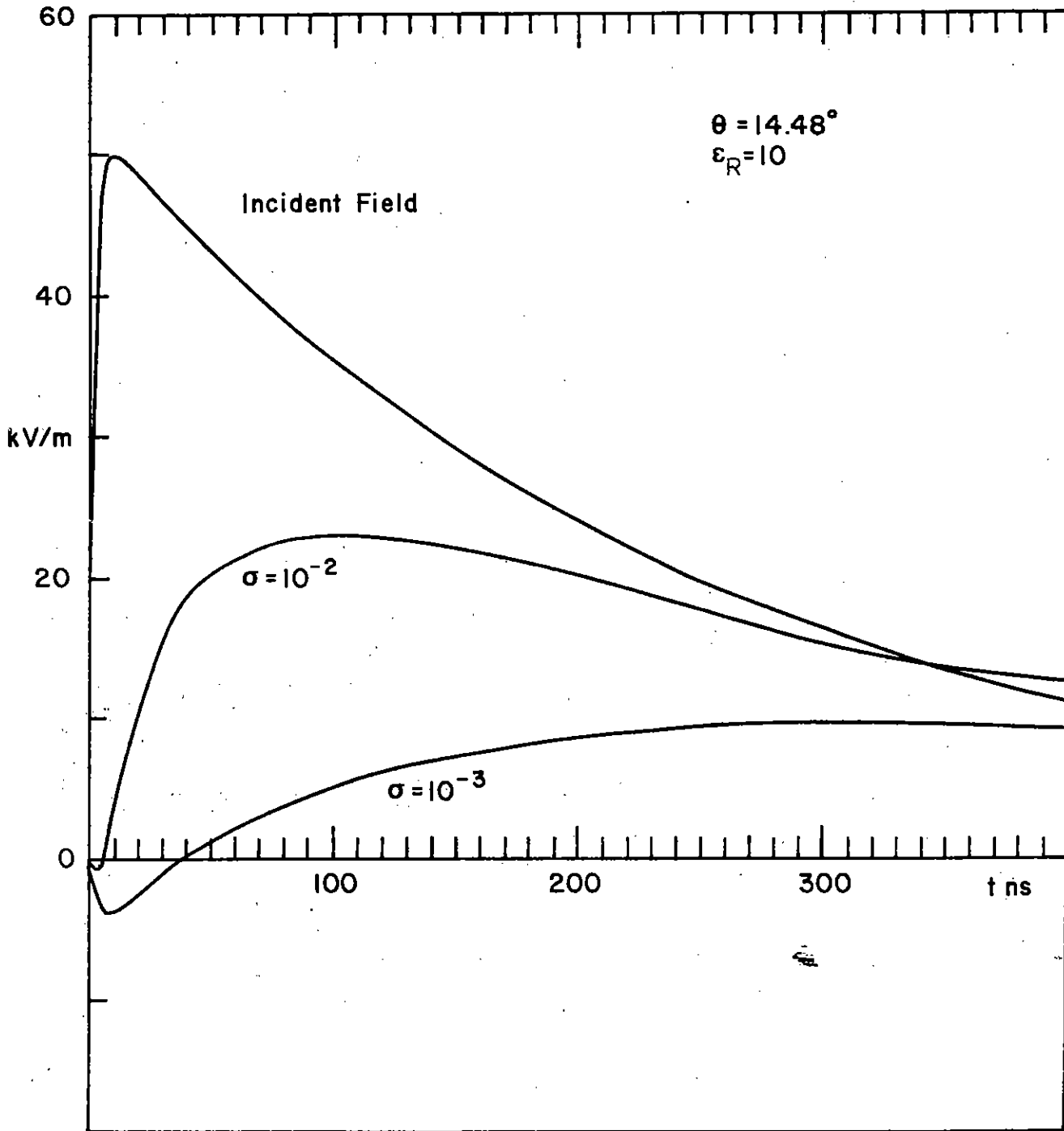


Figure 5. Reflected electric field (-):  $\epsilon_R = 10$ ,  $\theta = 14.48^\circ$ . The incident field is given by equation 10.

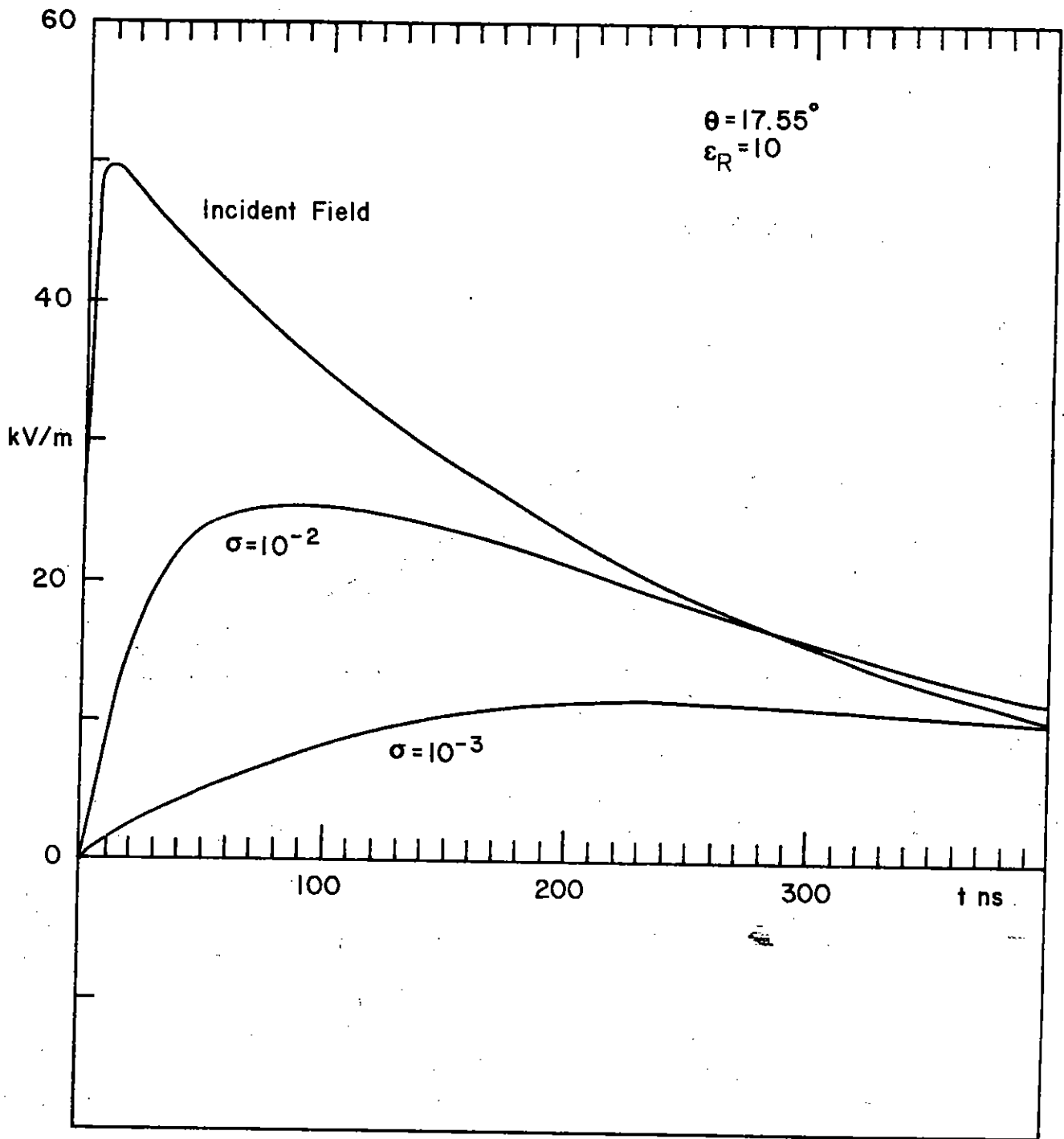


Figure 6. Reflected electric field (-):  $\epsilon_R = 10$ ,  $\theta = 17.55^\circ$ . The incident field is given by equation 10.

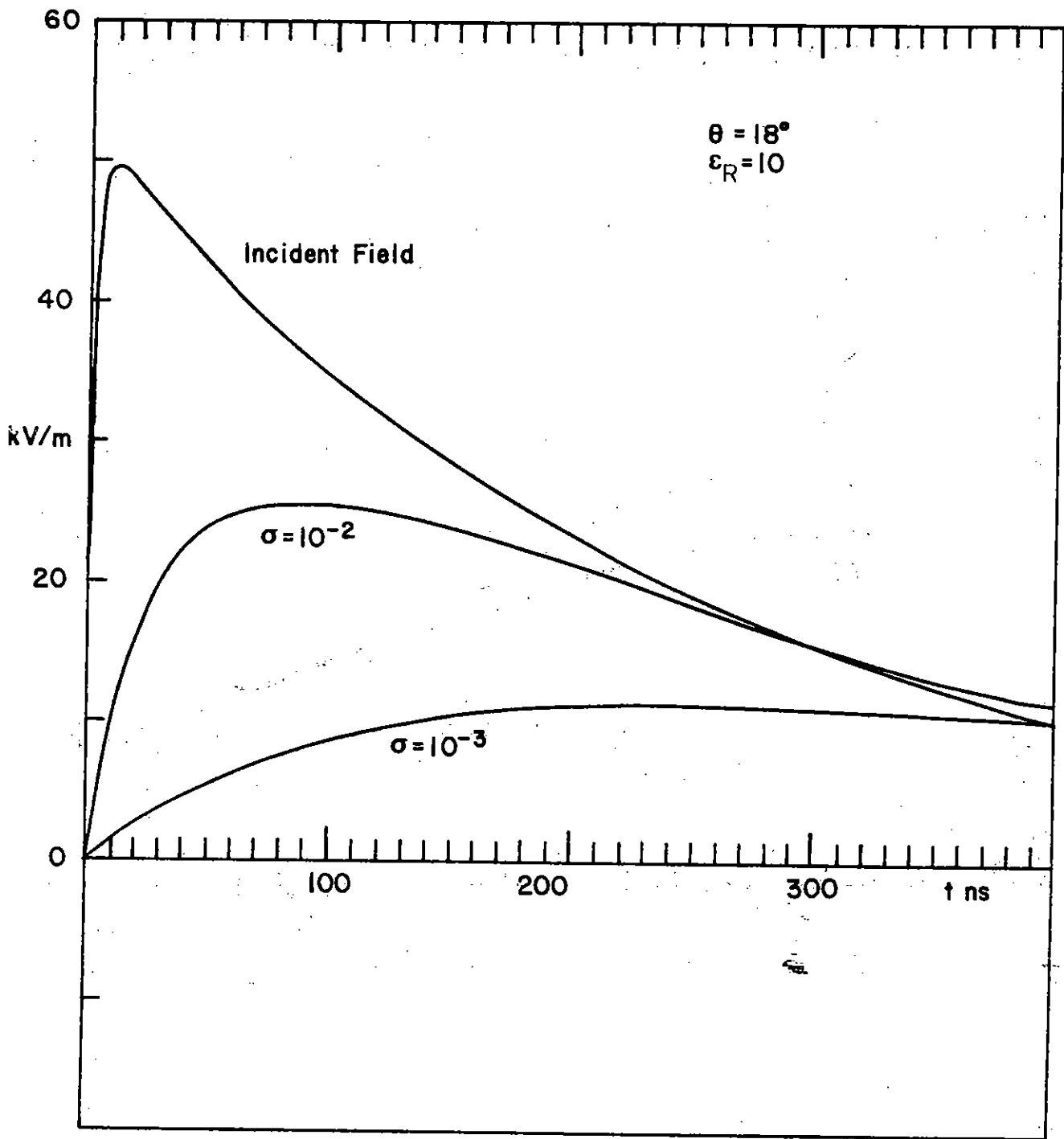


Figure 7. Reflected electric field (-):  $\epsilon_R = 10$ ,  $\theta = 18^\circ$ . The incident field is given by equation 10.

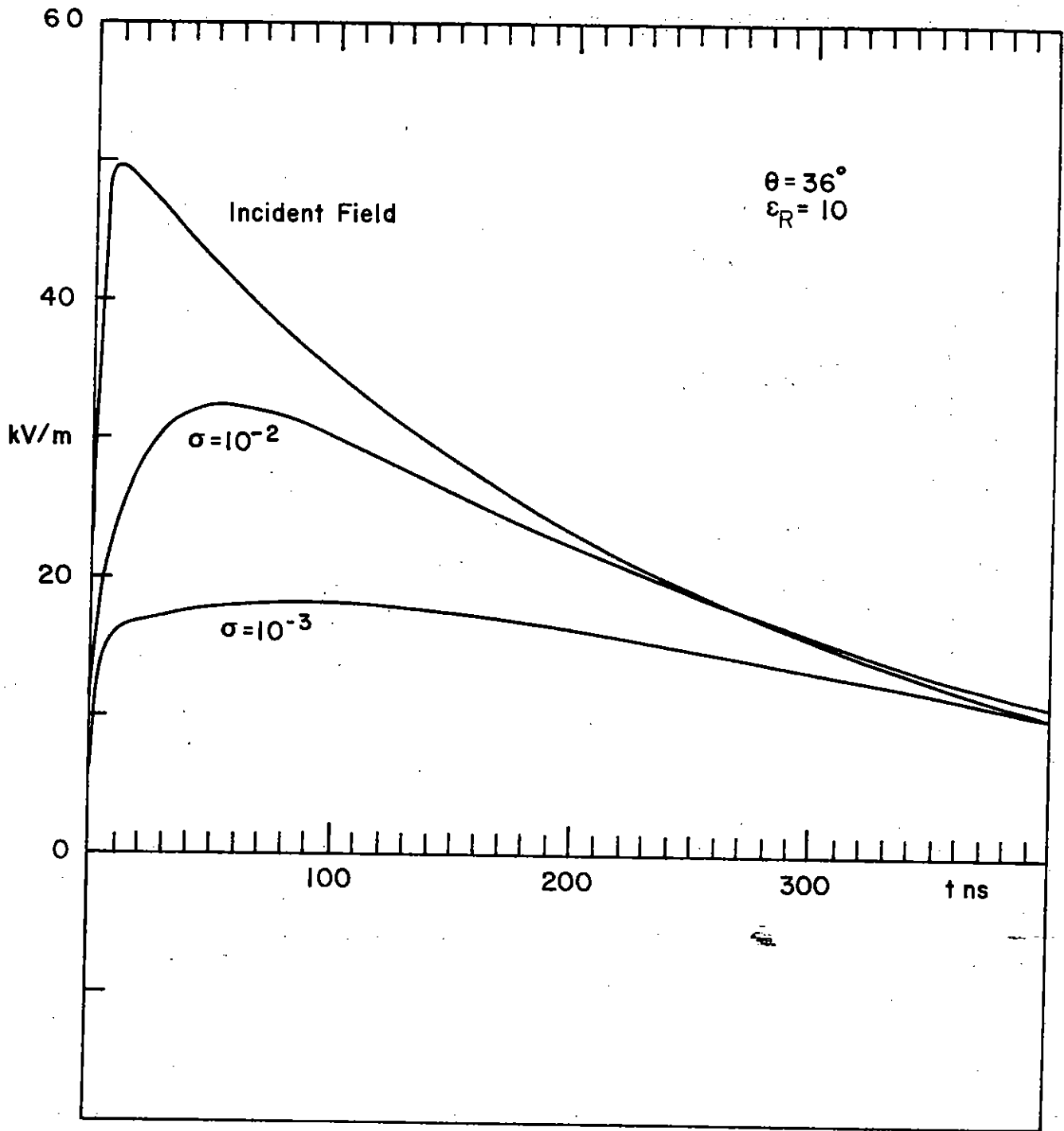


Figure 8. Reflected electric field (-):  $\epsilon_R = 10$ ,  $\theta = 36^\circ$ . The incident field is given by equation 10.

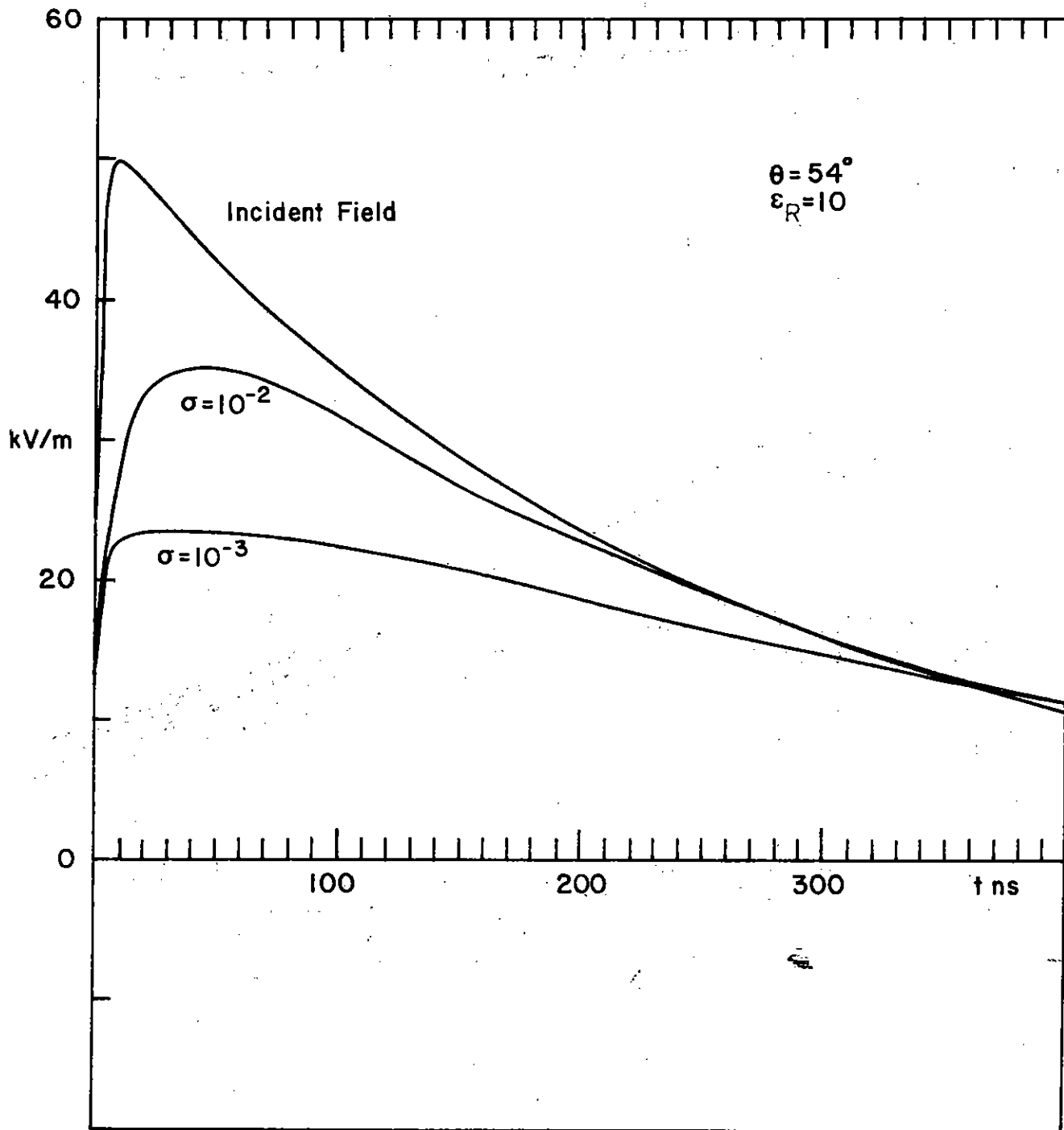


Figure 9. Reflected electric field (-):  $\epsilon_R = 10$ ,  $\theta = 54^\circ$ . The incident field is given by equation 10.



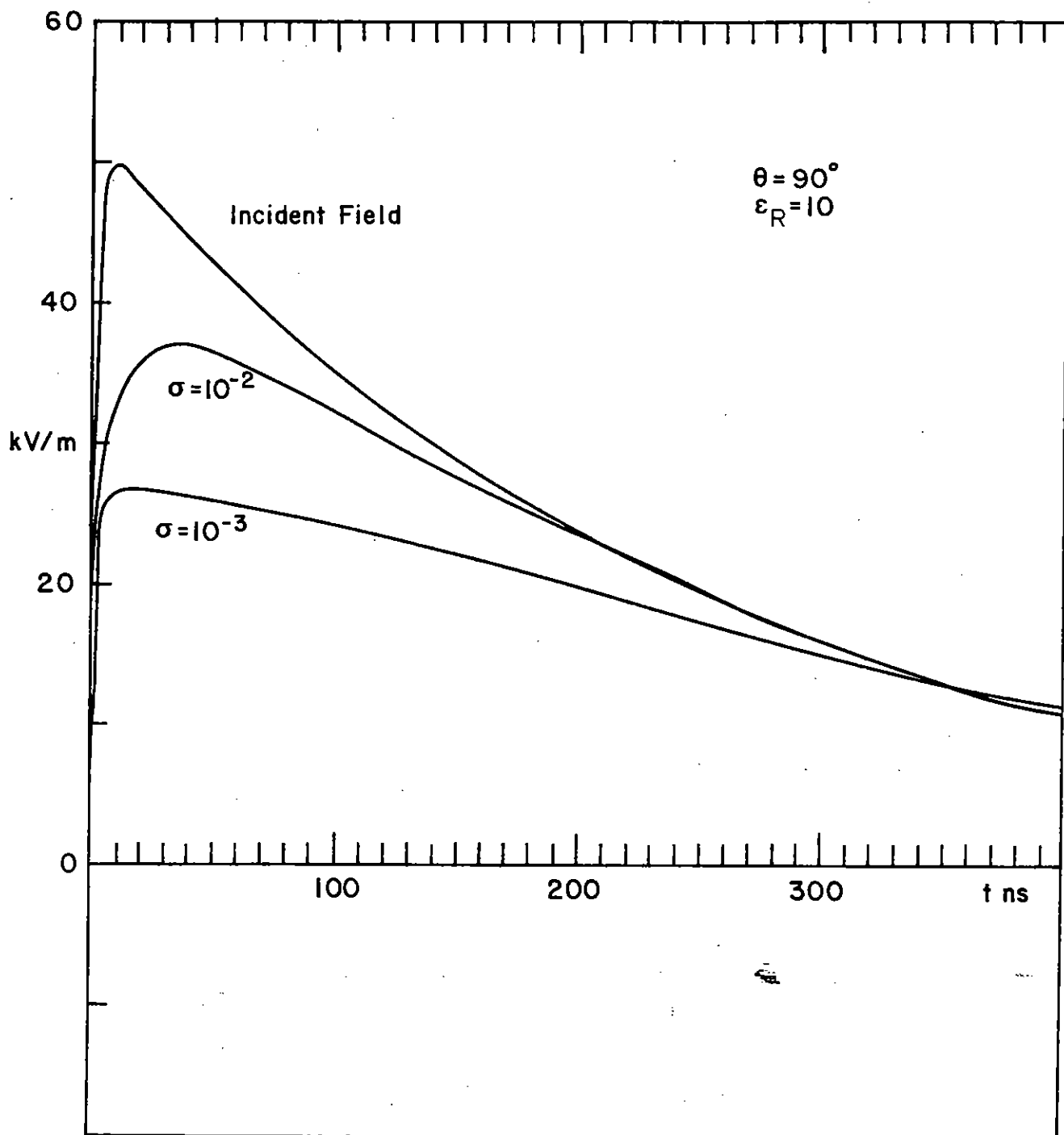


Figure 10. Reflected electric field (-):  $\epsilon_R = 10$ ,  $\theta = 90^\circ$ . The incident field is given by equation 10.

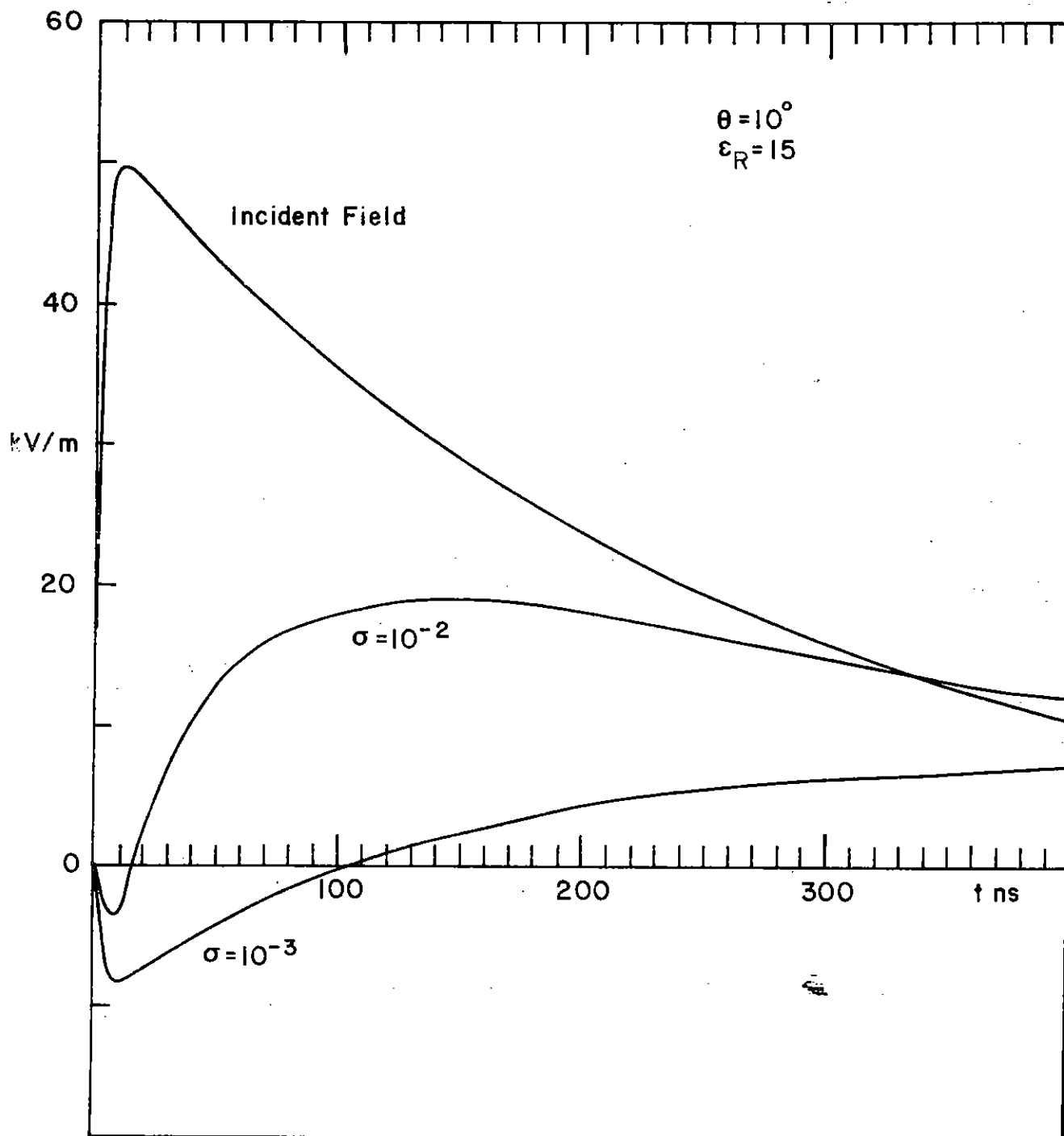


Figure 11. Reflected electric field (-):  $\epsilon_R = 15$ ,  $\theta = 10^\circ$ . The incident field is given by equation 10.

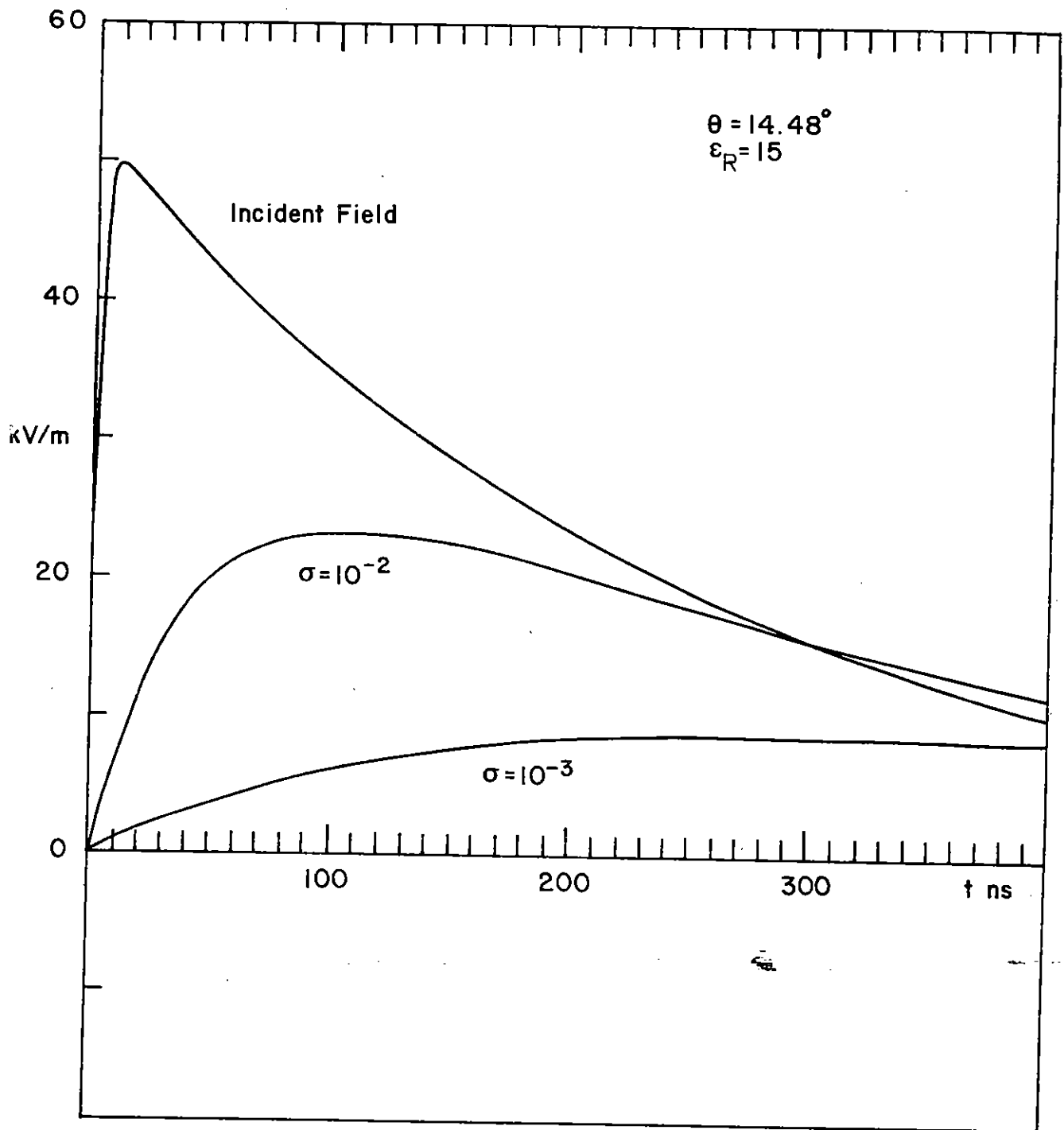


Figure 12. Reflected electric field (-):  $\epsilon_R = 15$ ,  $\theta = 14.48^\circ$ . The incident field is given by equation 10.

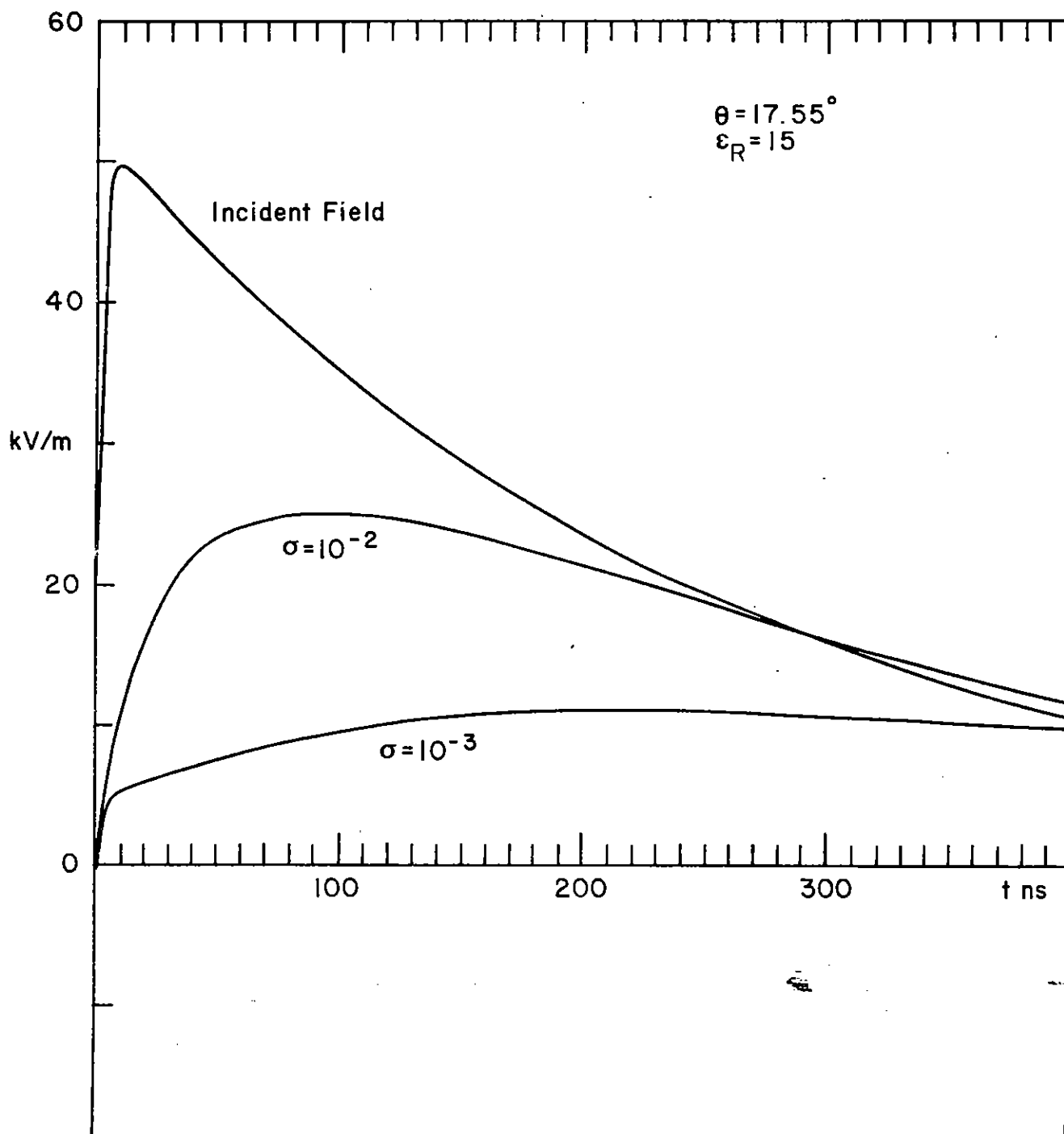


Figure 13. Reflected electric field (-):  $\epsilon_R = 15$ ,  $\theta = 17.55^\circ$ . The incident field is given by equation 10.

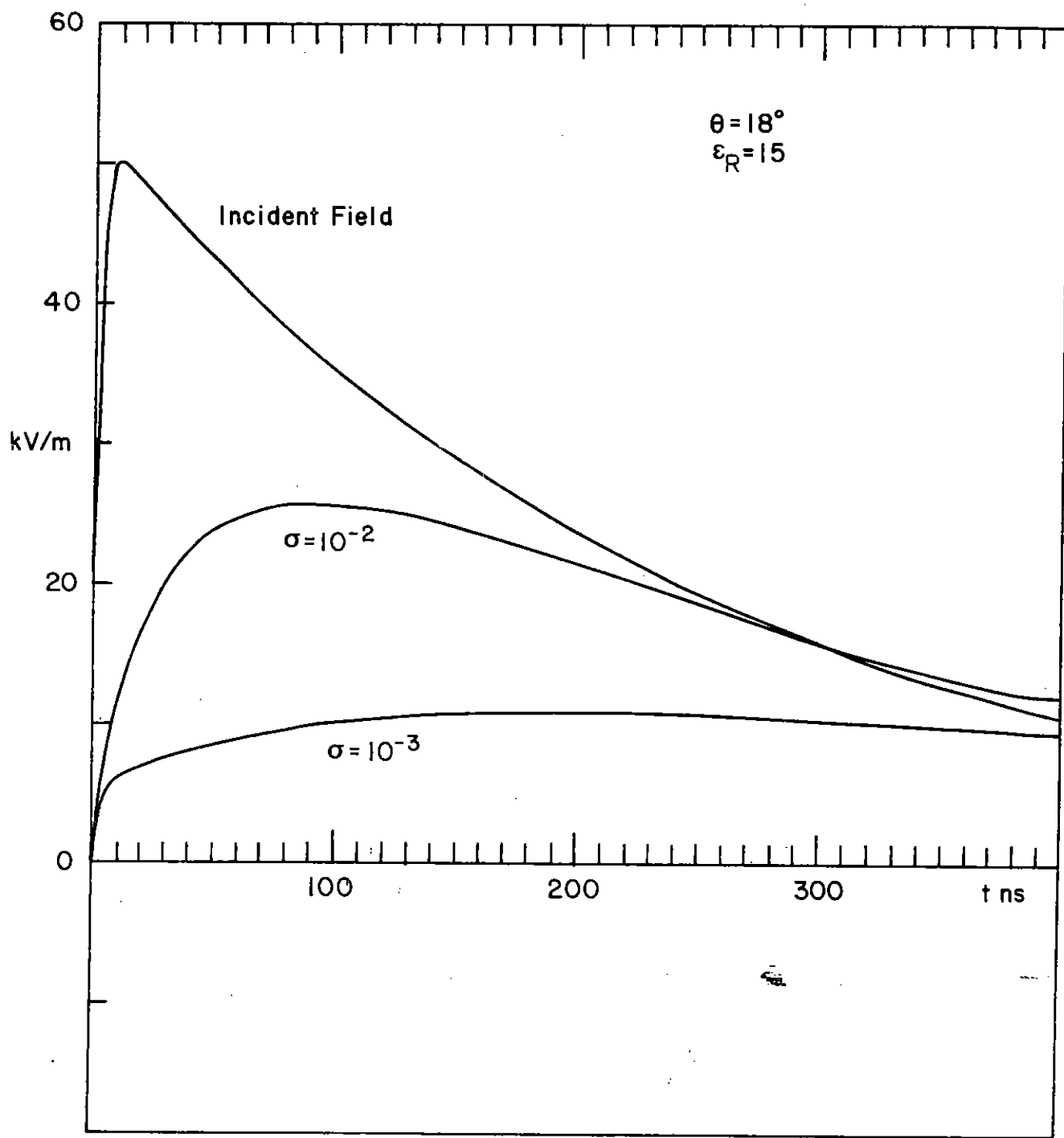


Figure 14. Reflected electric field (-):  $\epsilon_R = 15$ ,  $\theta = 18^\circ$ . The incident field is given by equation 10.

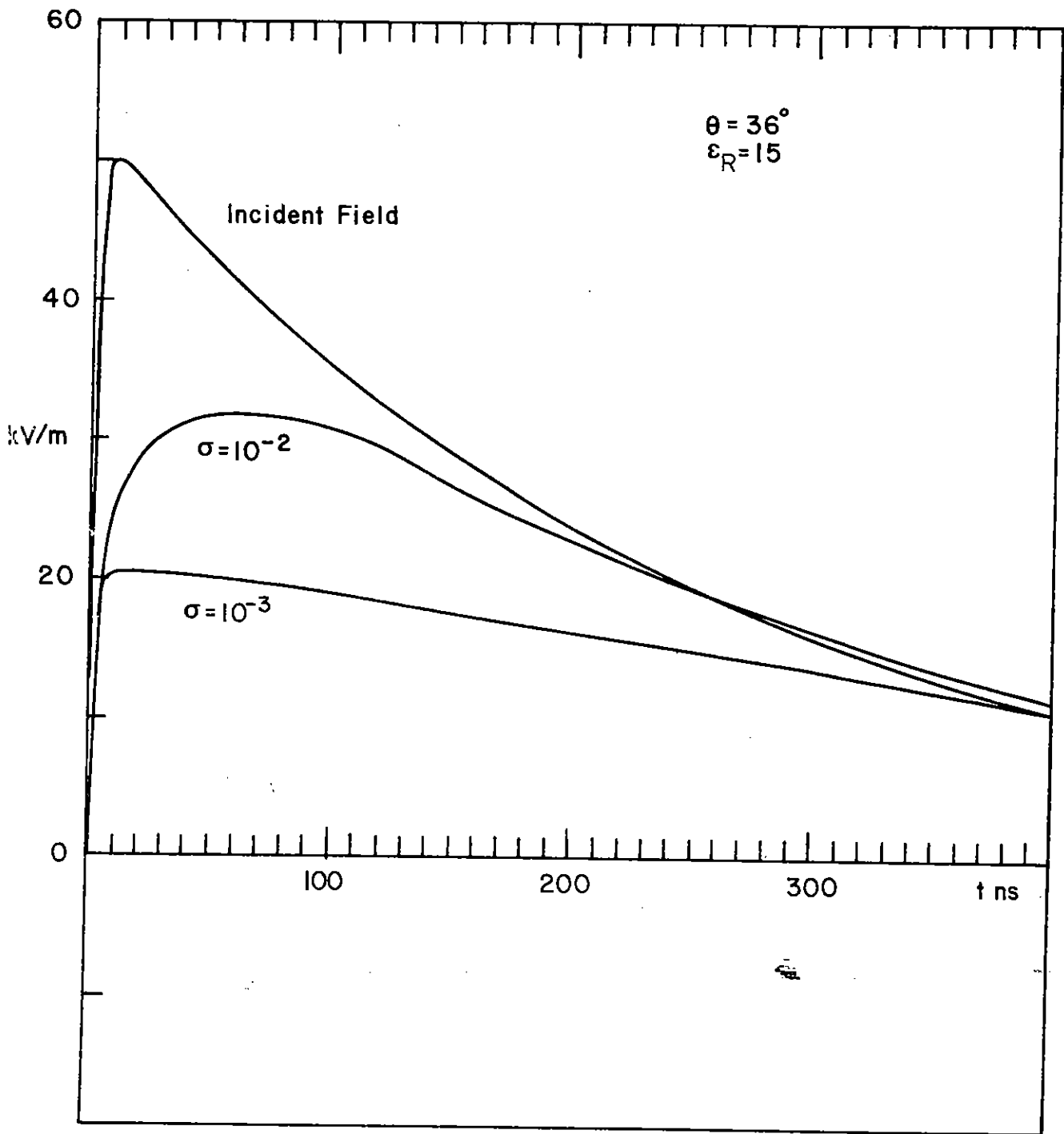


Figure 15. Reflected electric field (-):  $\epsilon_R = 15$ ,  $\theta = 36^\circ$ . The incident field is given by equation 10.

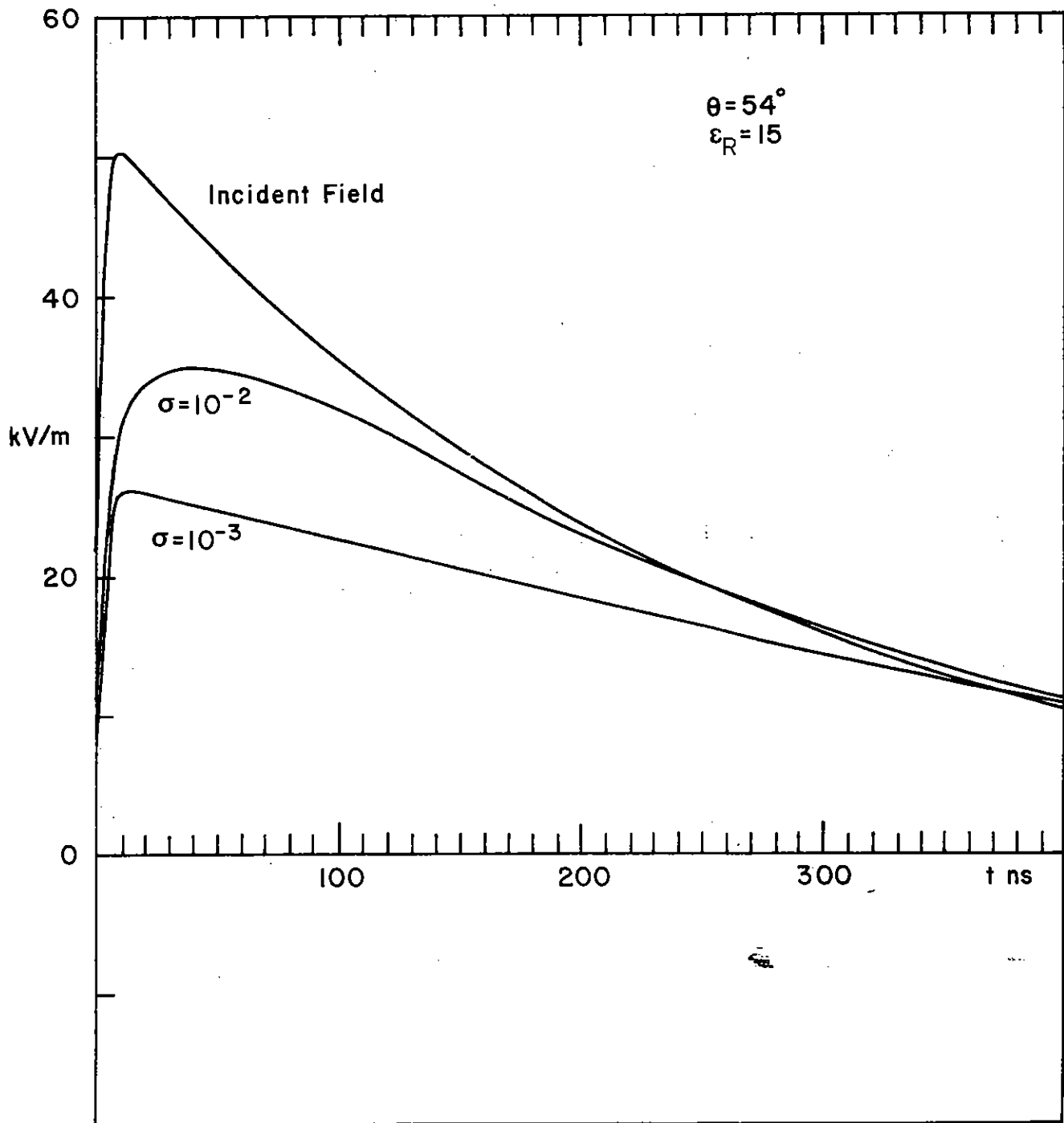


Figure 16. Reflected electric field (-):  $\epsilon_R = 15$ ,  $\theta = 54^\circ$ . The incident field is given by equation 10.

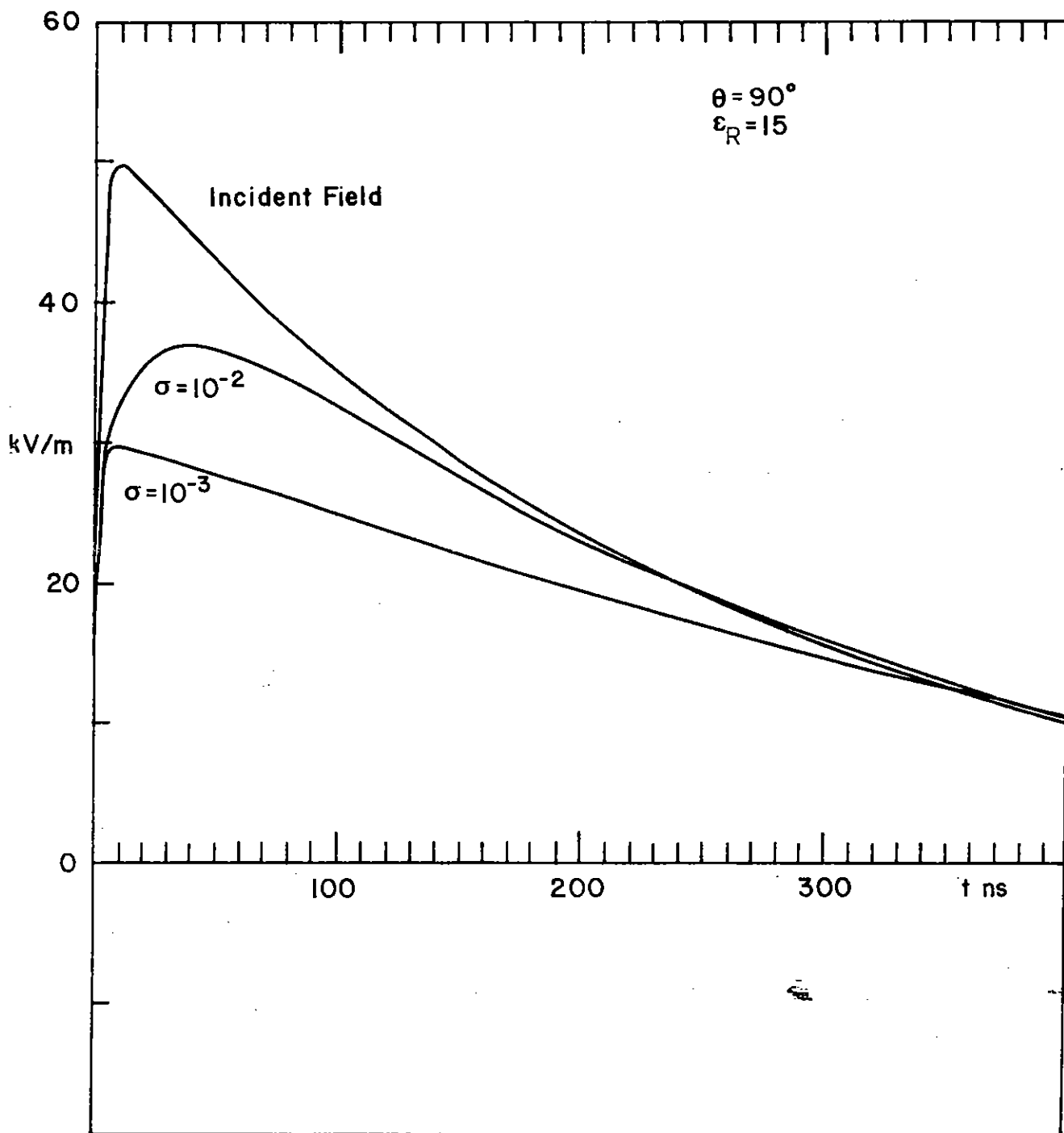


Figure 17. Reflected electric field (-):  $\epsilon_R = 15$ ,  $\theta = 90^\circ$ . The incident field is given by equation 10.



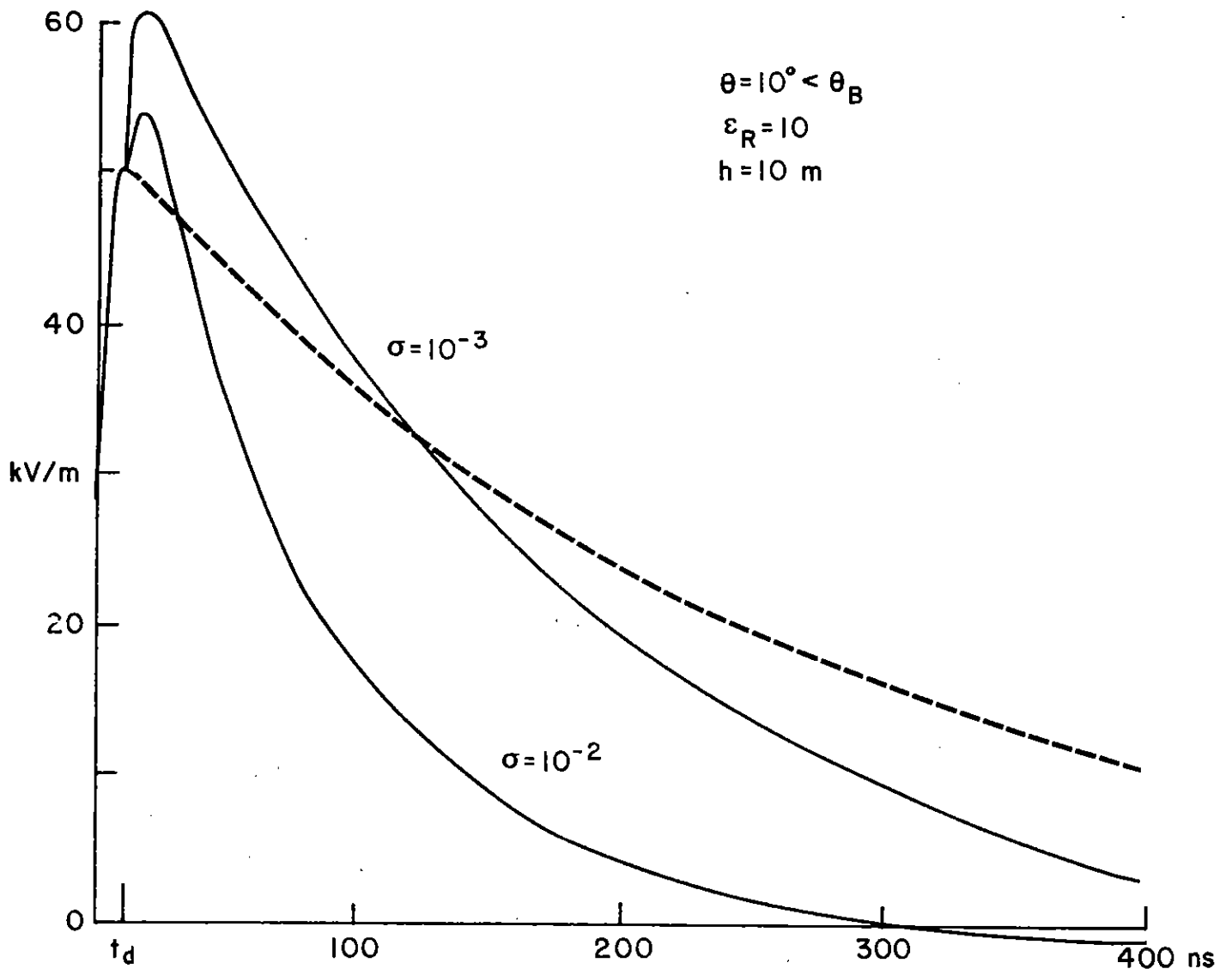


Figure 18. Composite field for  $h = 10 \text{ m}$ ,  $\epsilon_R = 10$  and  $\theta = 10^\circ$ .

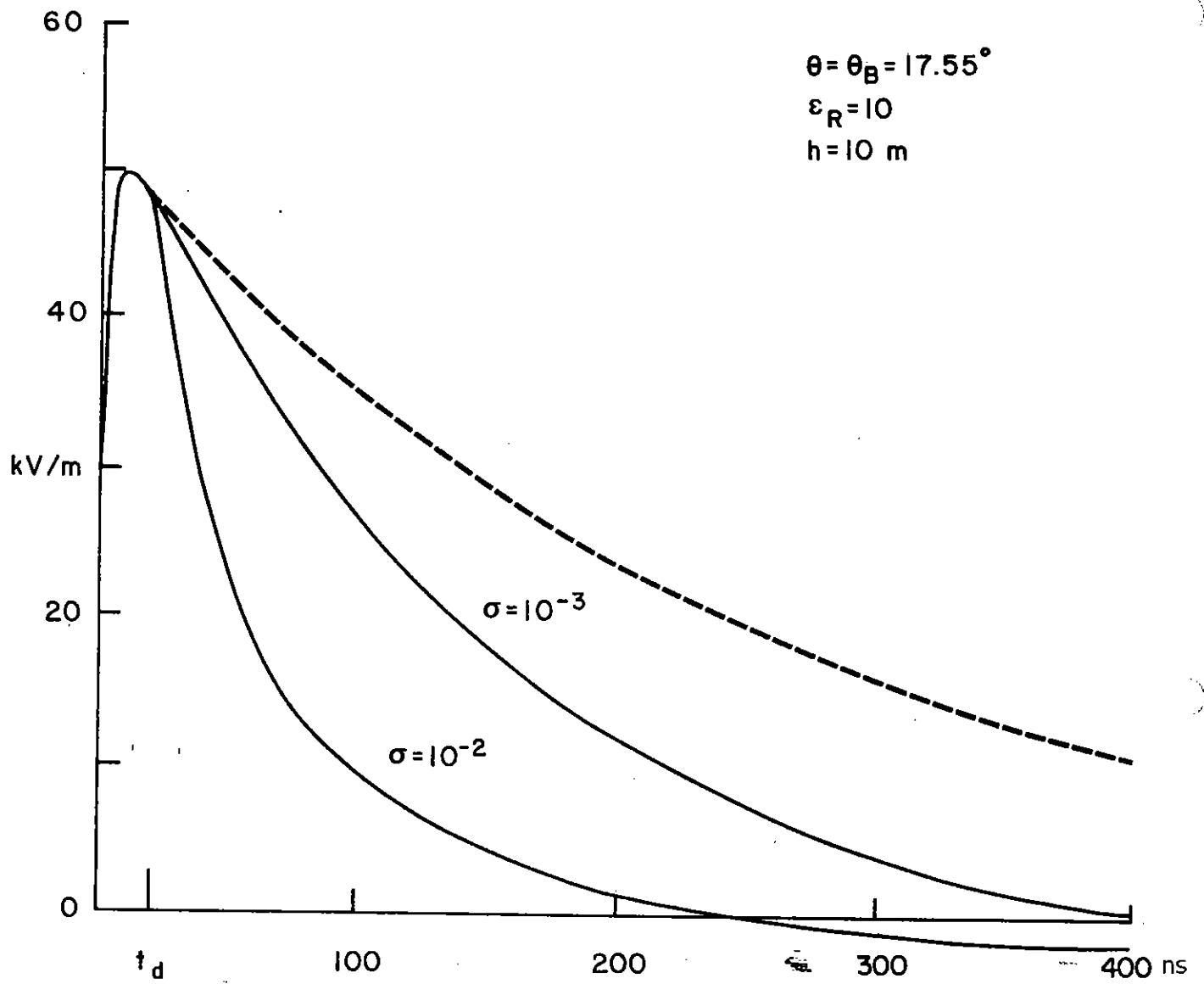


Figure 19. Composite field for  $h = 10 \text{ m}$ ,  $\epsilon_R = 10$  and  $\theta = 17.55^\circ$ .

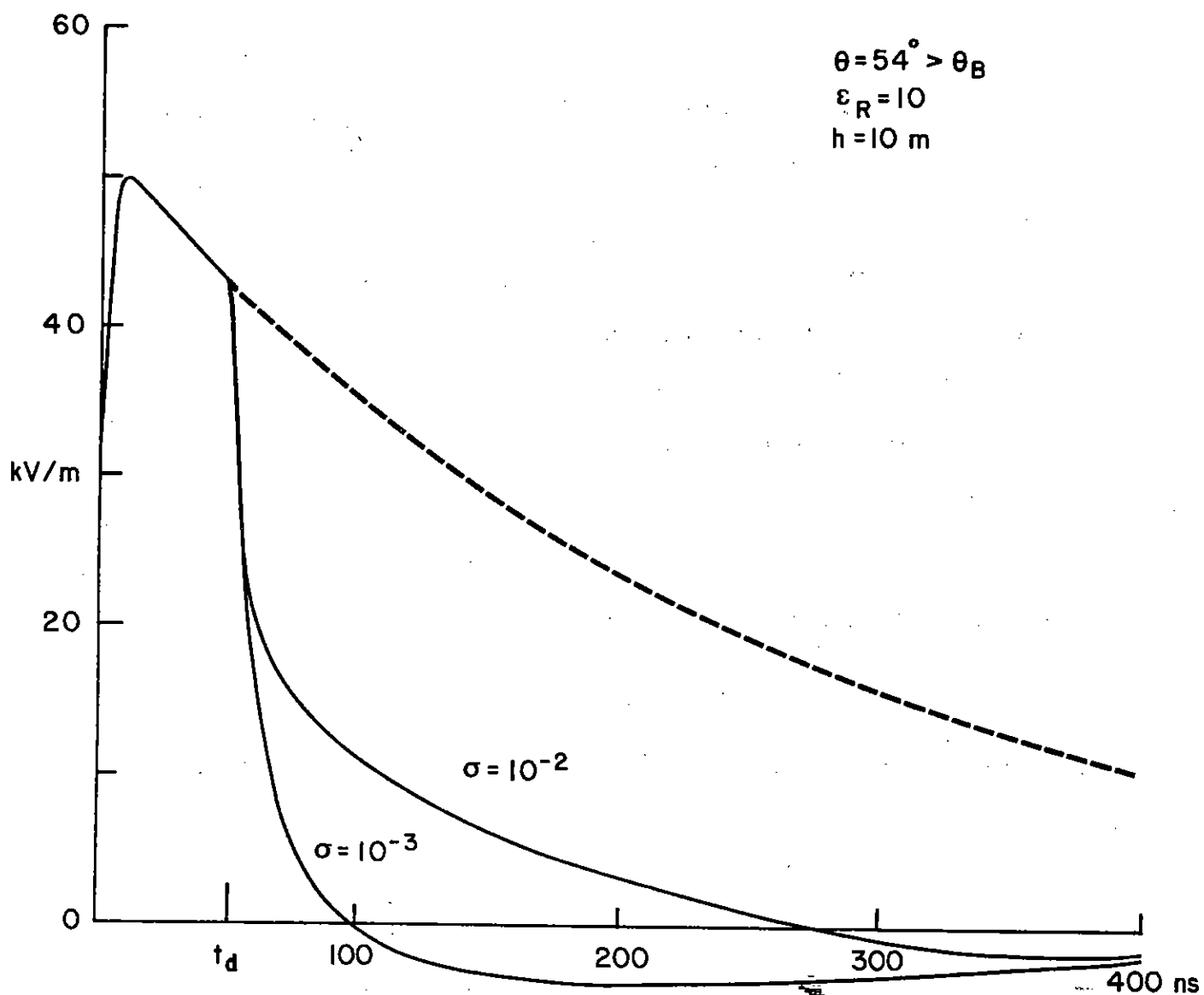


Figure 20. Composite field for  $h = 10 \text{ m}$ ,  $\epsilon_R = 10$  and  $\theta = 54^\circ$ .

clear from Figure 18 ( $0 < \beta_B$ ) that the composite field is greater than the incident field, particularly so for the smaller conductivity ( $\sigma = 10^{-3}$ ). Notice also that the composite field is relatively small for  $t > 400$  ns in all three cases.

The unit-step response for the reflected wave was also calculated for the purpose of comparison with the work of Baum [2]. The results are given in Figures 21 through 34 where the same parameters are used as were used in Figures 4 through 17. Notice that the negative of the step response is actually shown. Also, notice that

$$E_r(0) = \frac{\beta - 1}{\beta + 1} \quad (t = 0)$$

from the initial-value theorem, and

$$E_r(\infty) = -1 \quad (t \rightarrow \infty)$$

from the final-value theorem. The results are in very good agreement with those of Baum, and Figure 25 was chosen as an example to demonstrate this.

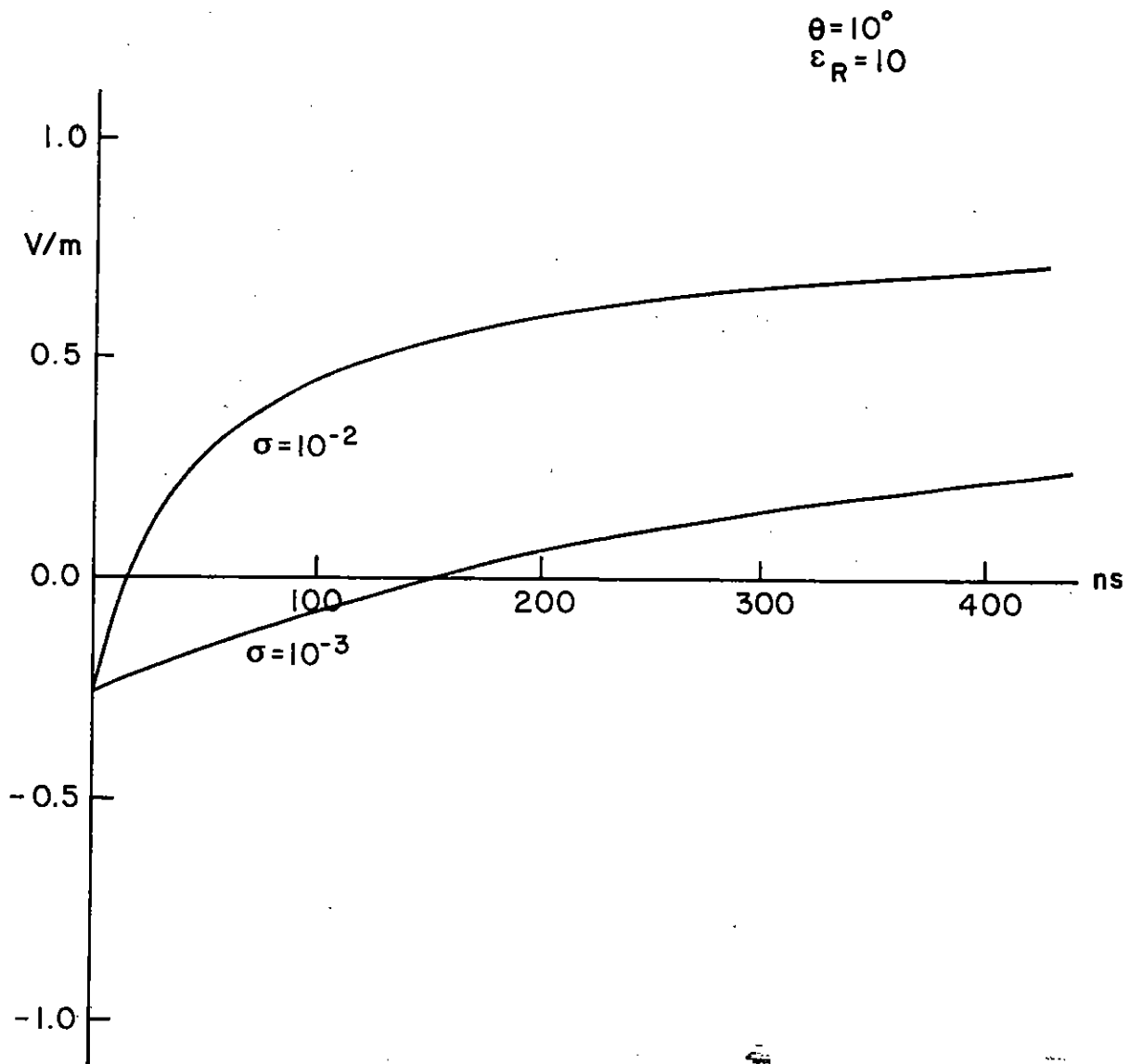


Figure 21. Unit-step response, reflected field:  $\epsilon_R = 10$ ,  $\theta = 10^\circ$ .

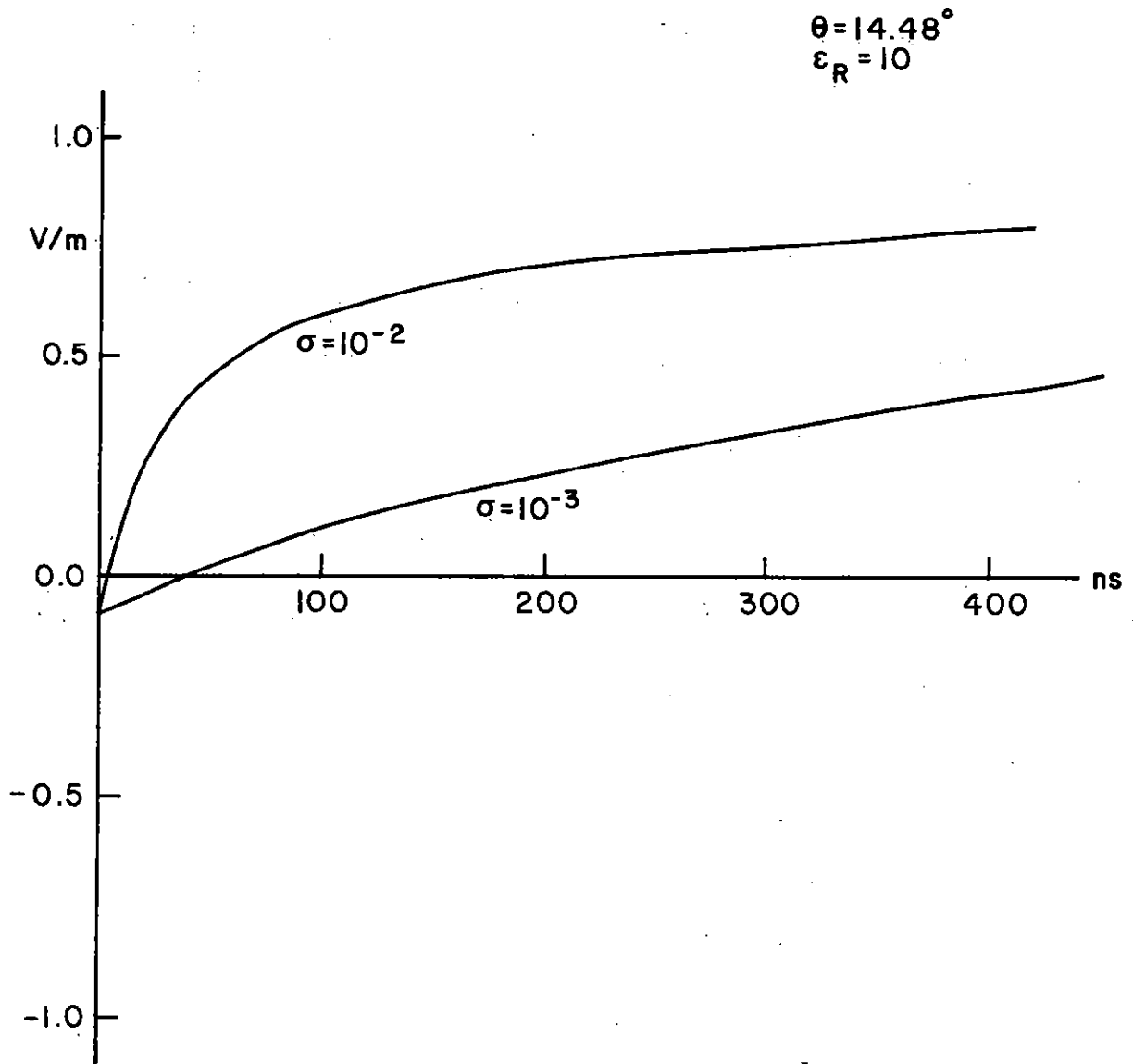


Figure 22. Unit-step response, reflected field:  $\epsilon_R = 10$ ,  $\theta = 14.48^\circ$ .

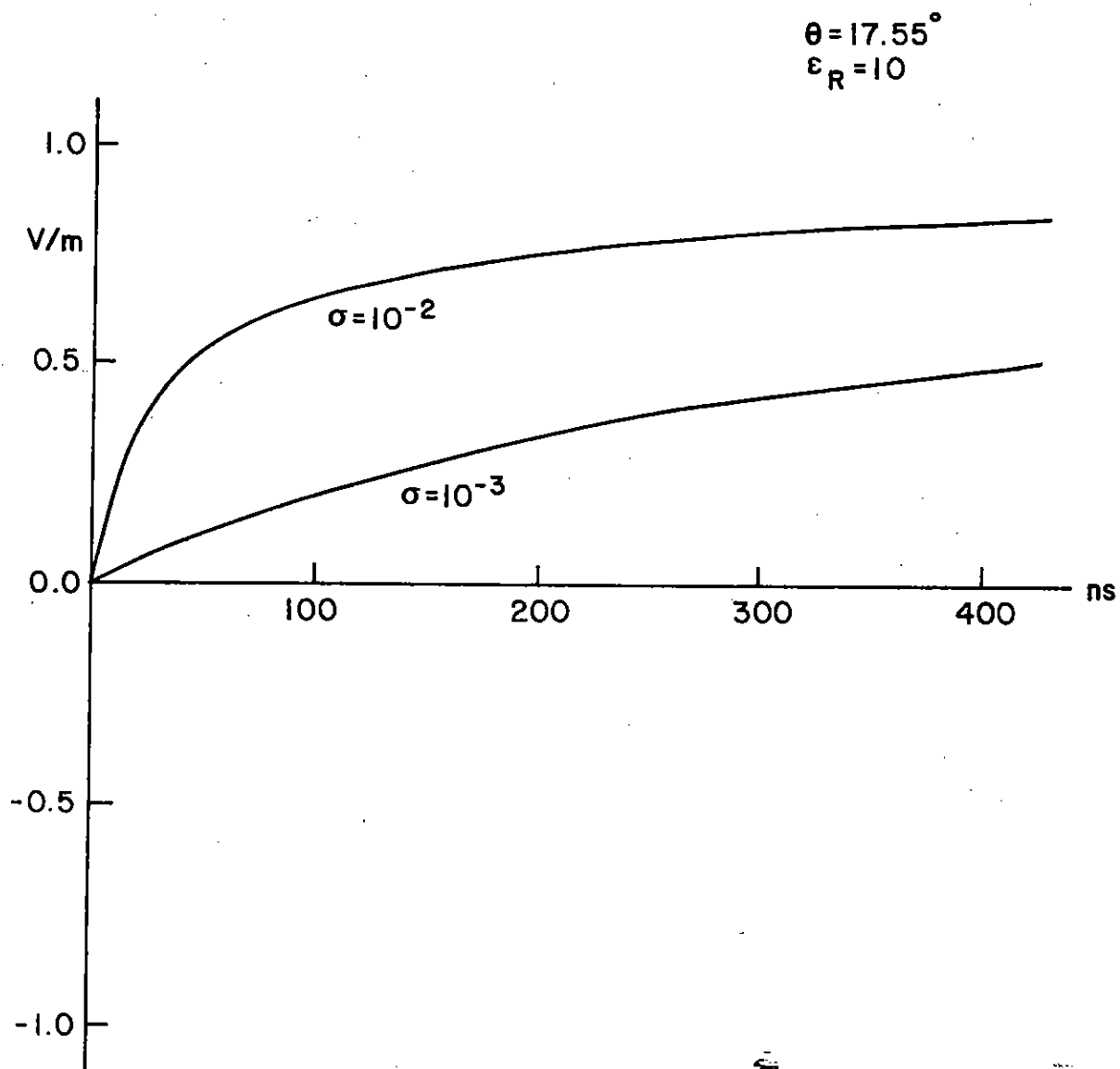


Figure 23. Unit-step response, reflected field:  $\epsilon_R = 10$ ,  $\theta = 17.55^\circ$ .

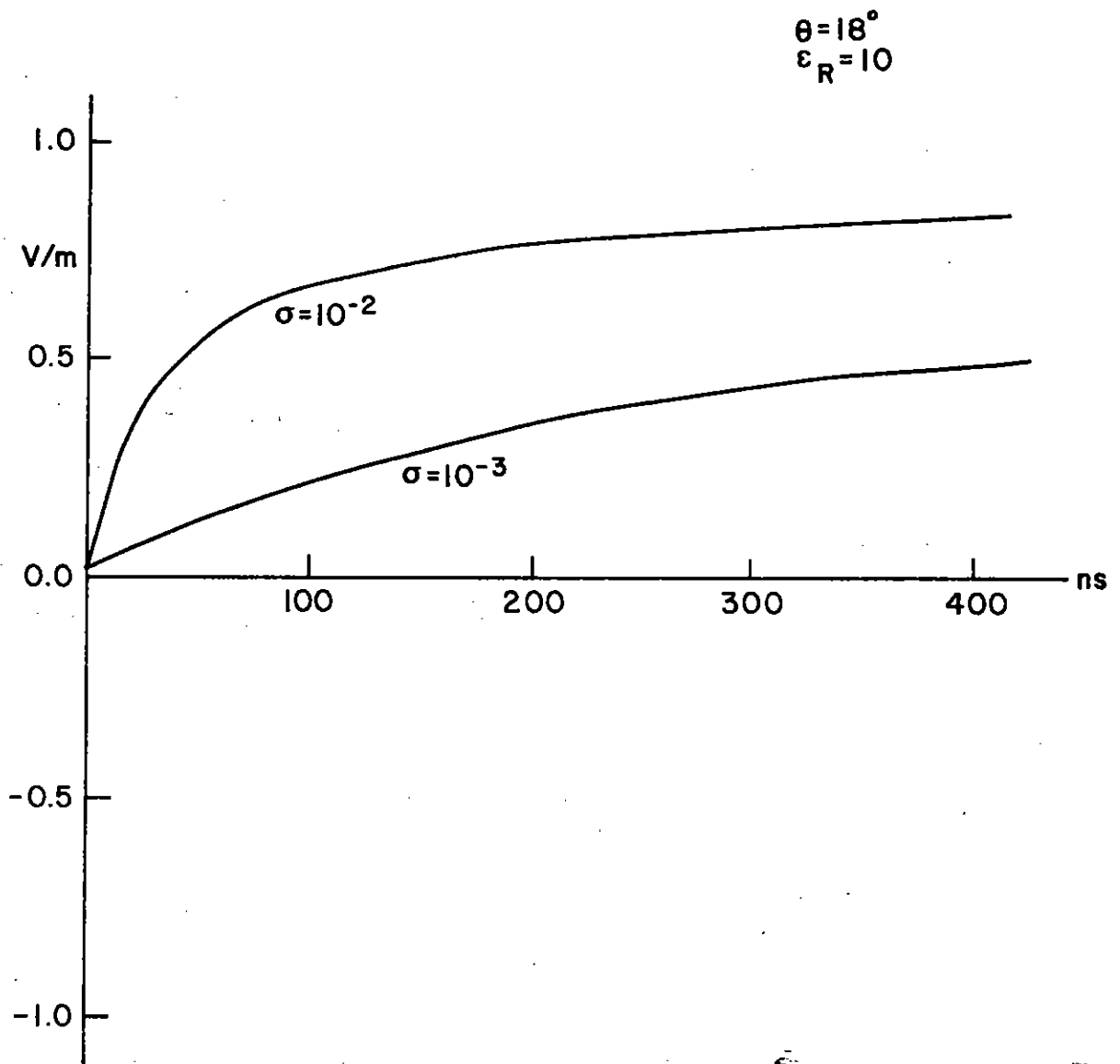


Figure 24. Unit-step response, reflected field:  $\epsilon_R = 10$ ,  $\theta = 18^\circ$ .



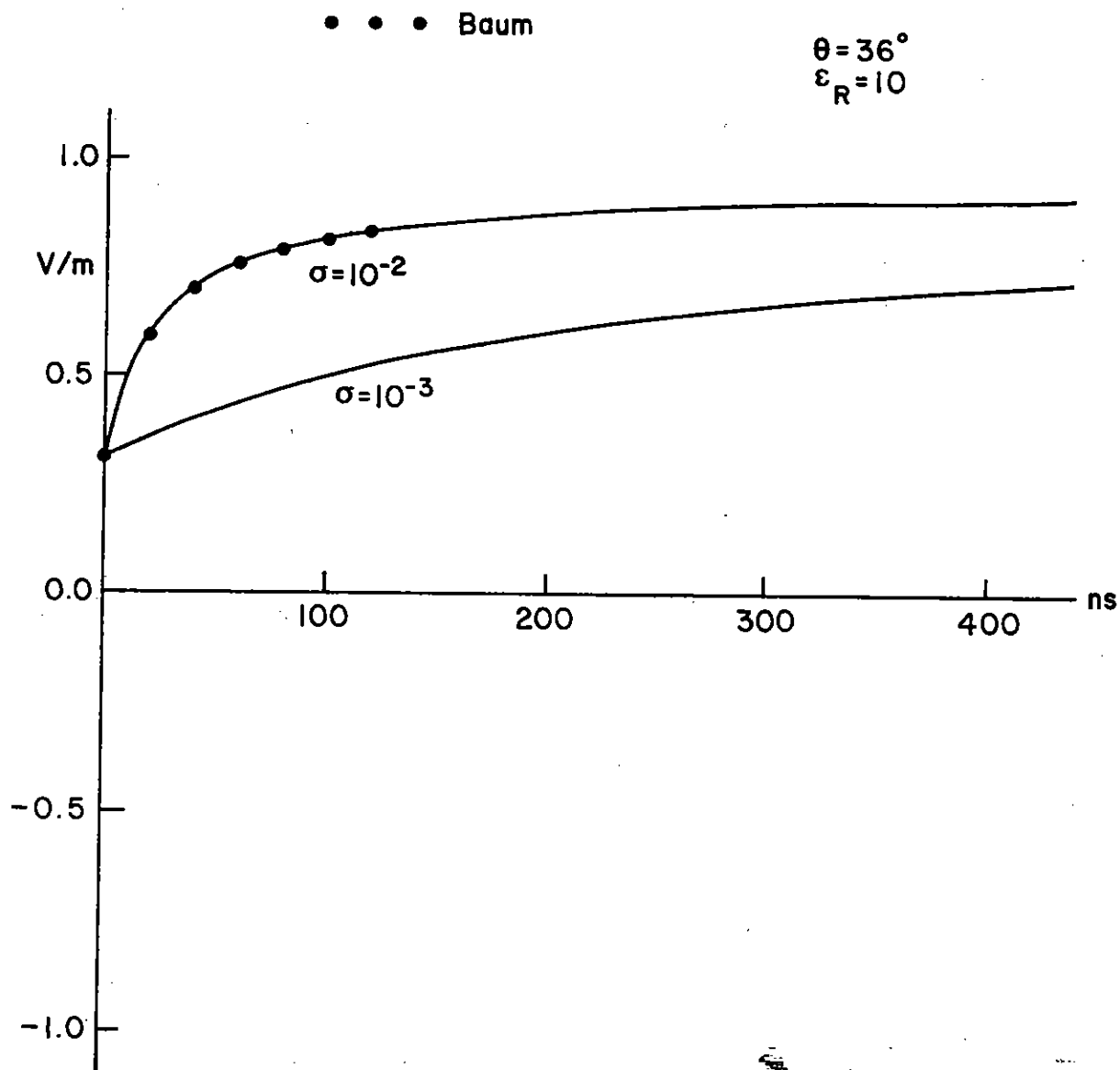


Figure 25. Unit-step response, reflected field:  $\epsilon_R = 10$ ,  $\theta = 36^\circ$ .

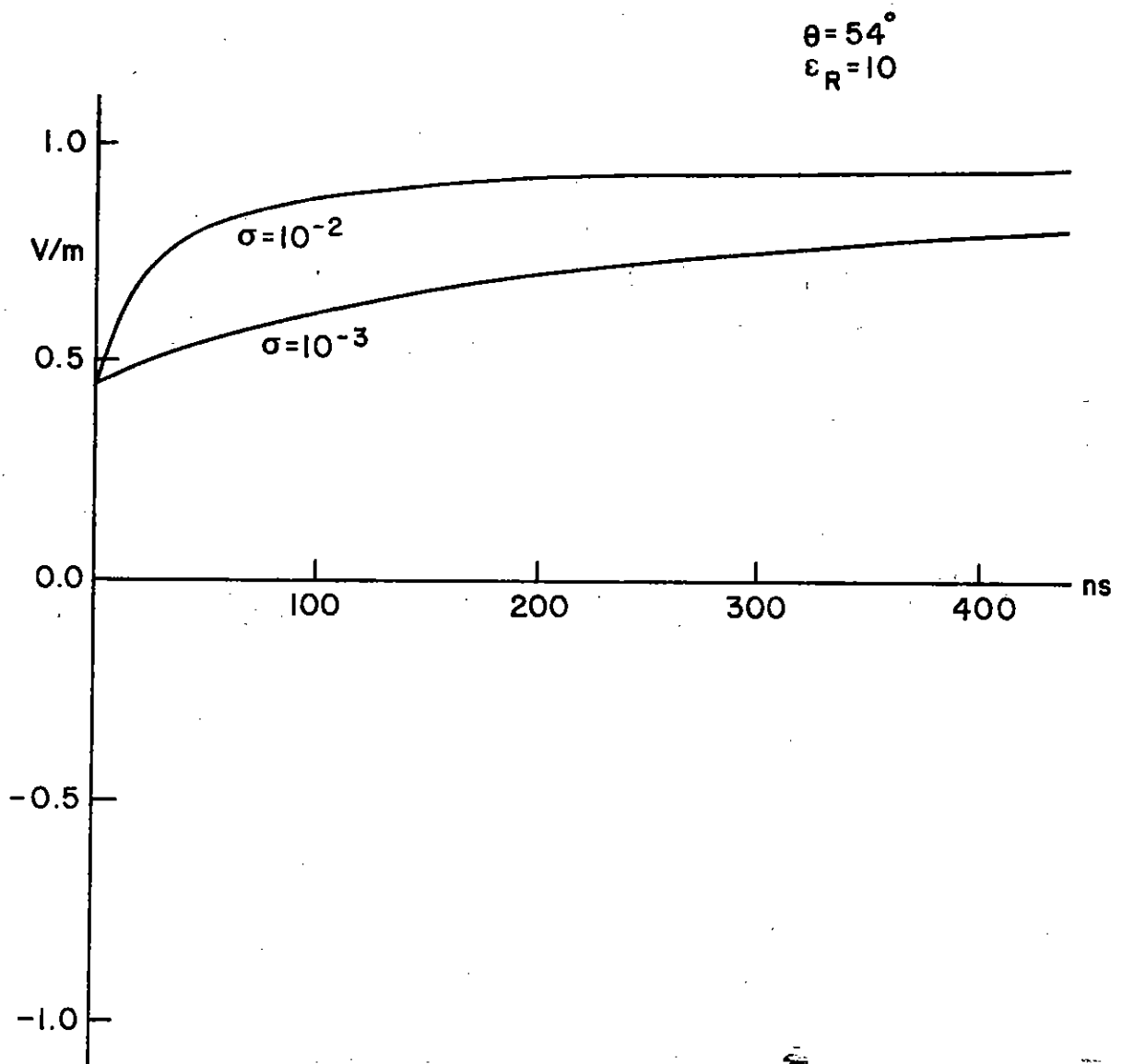


Figure 26. Unit-step response, reflected field:  $\epsilon_R = 10$ ,  $\theta = 54^\circ$ .

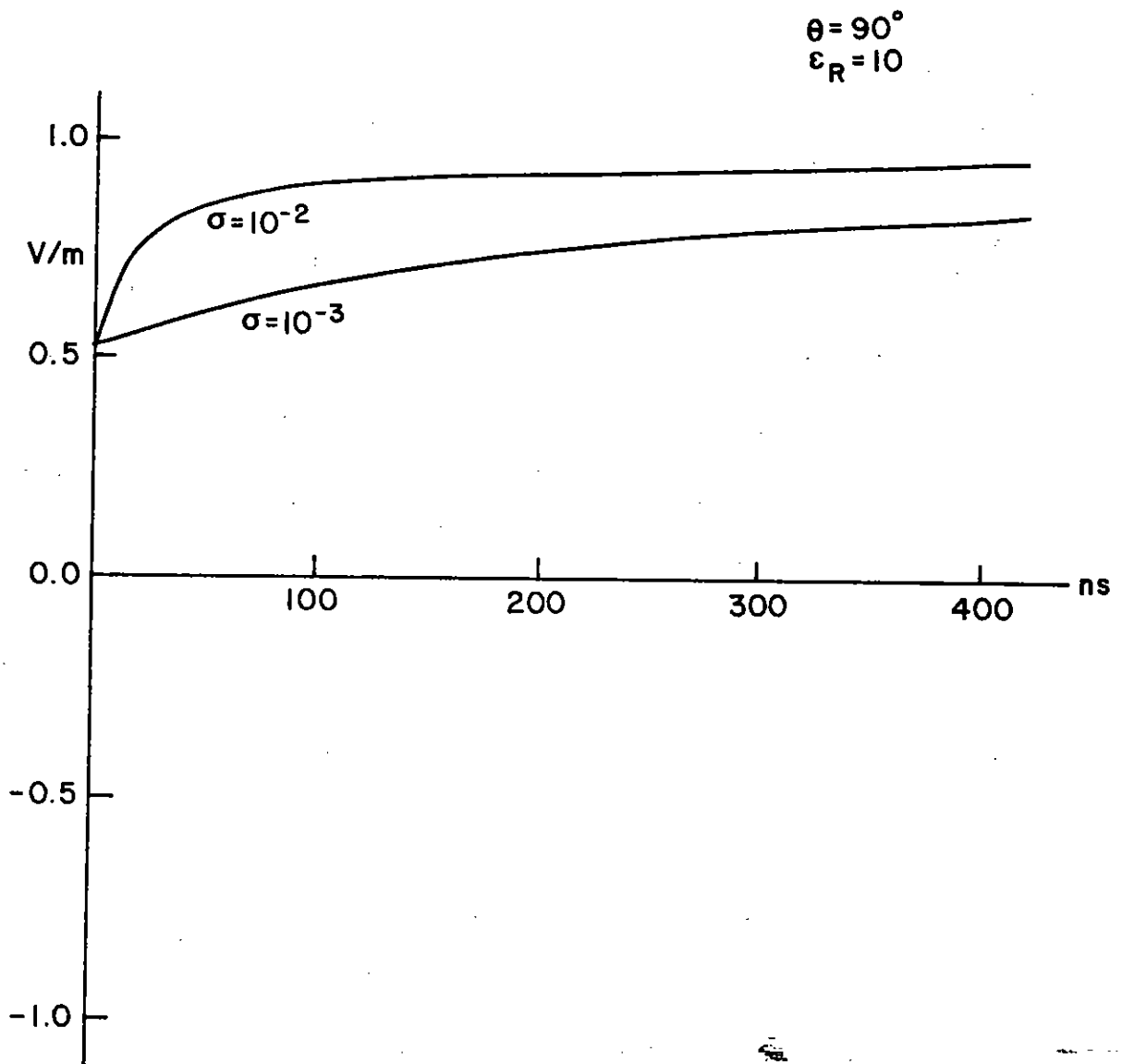


Figure 27. Unit-step response, reflected field:  $\epsilon_R = 10$ ,  $\theta = 90^\circ$ .

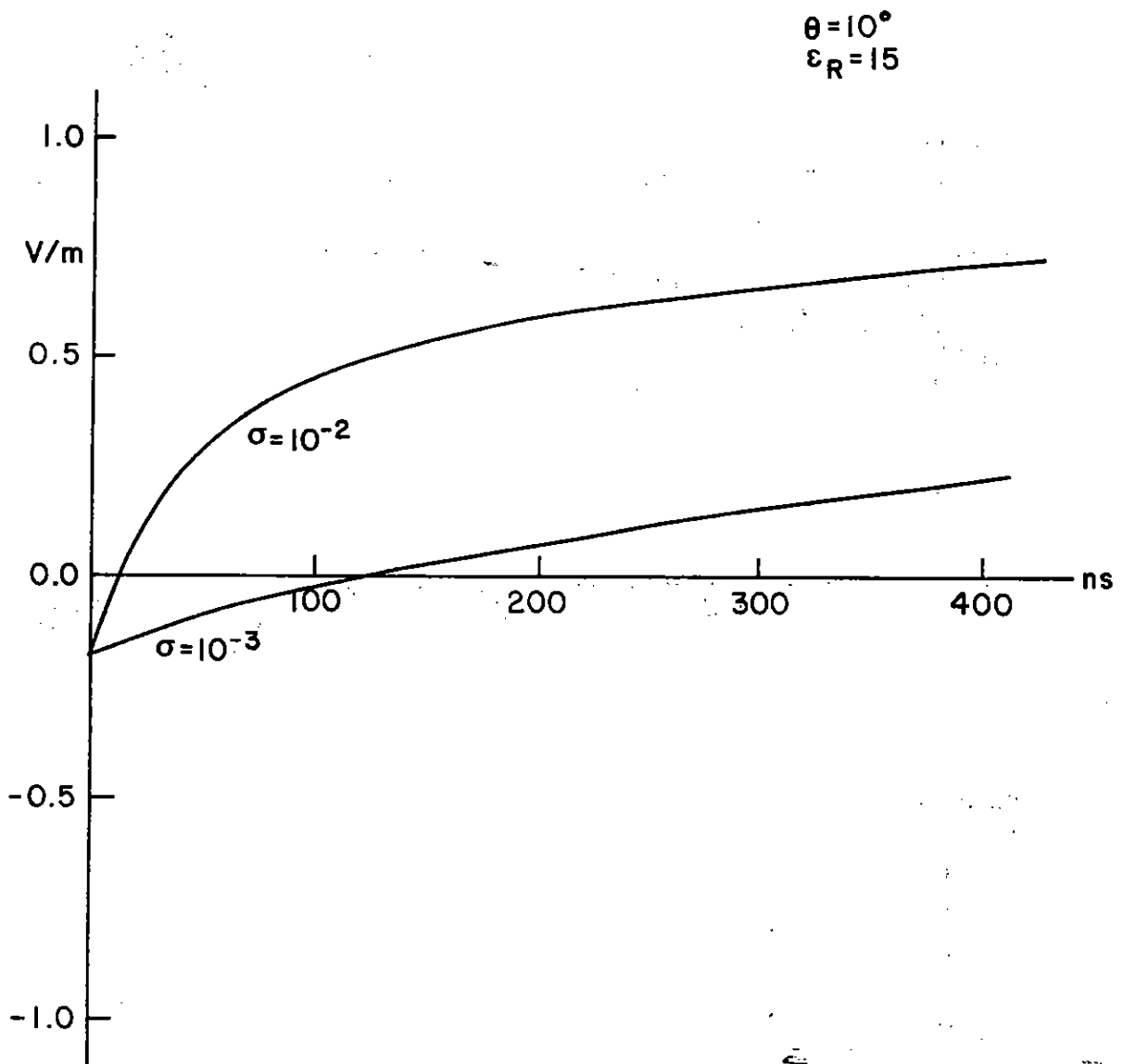


Figure 28. Unit-step response, reflected field:  $\epsilon_R = 15$ ,  $\theta = 10^\circ$ .

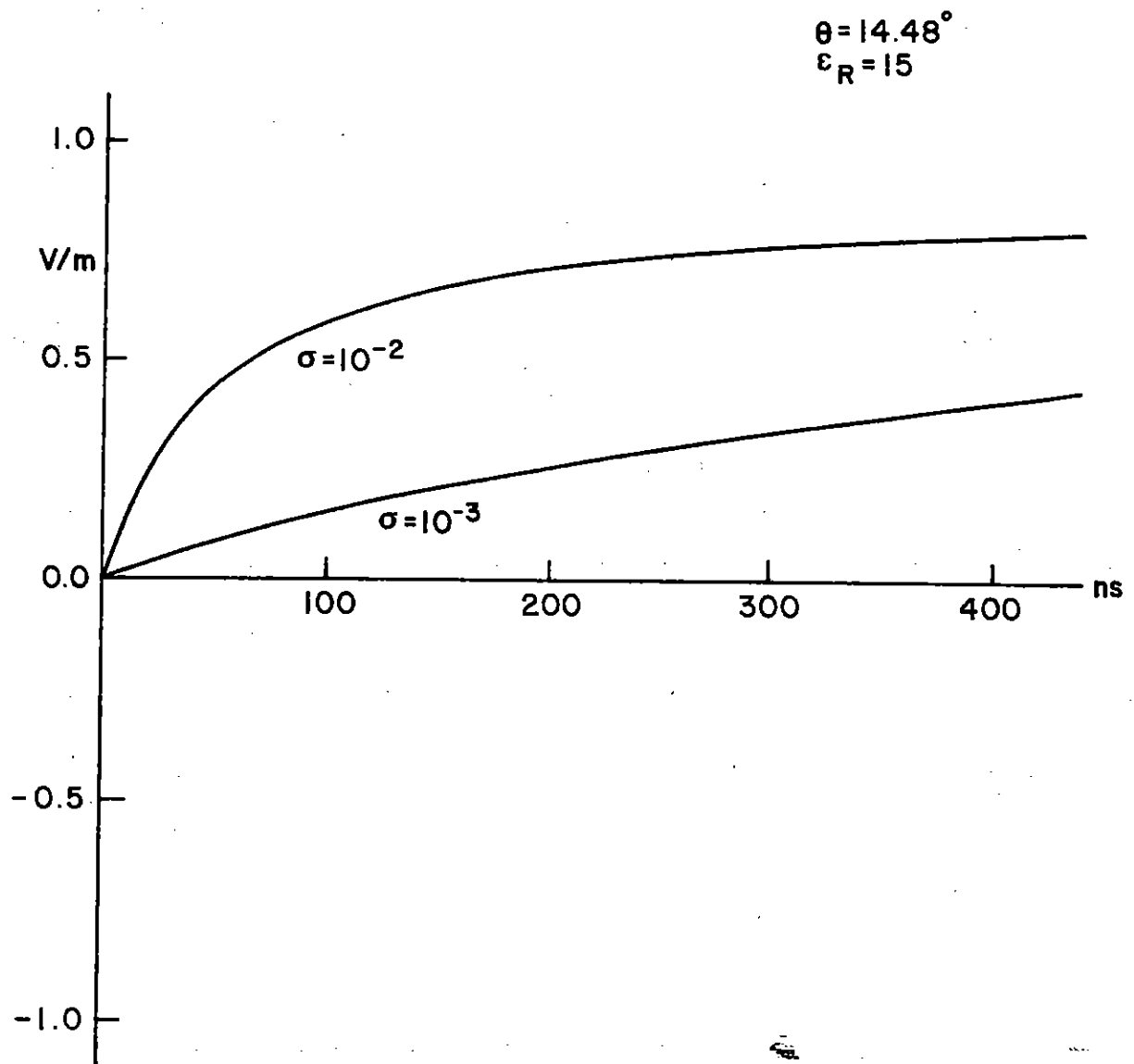


Figure 29. Unit-step response, reflected field:  $\epsilon_R = 15$ ,  $\theta = 14.48^\circ$ .

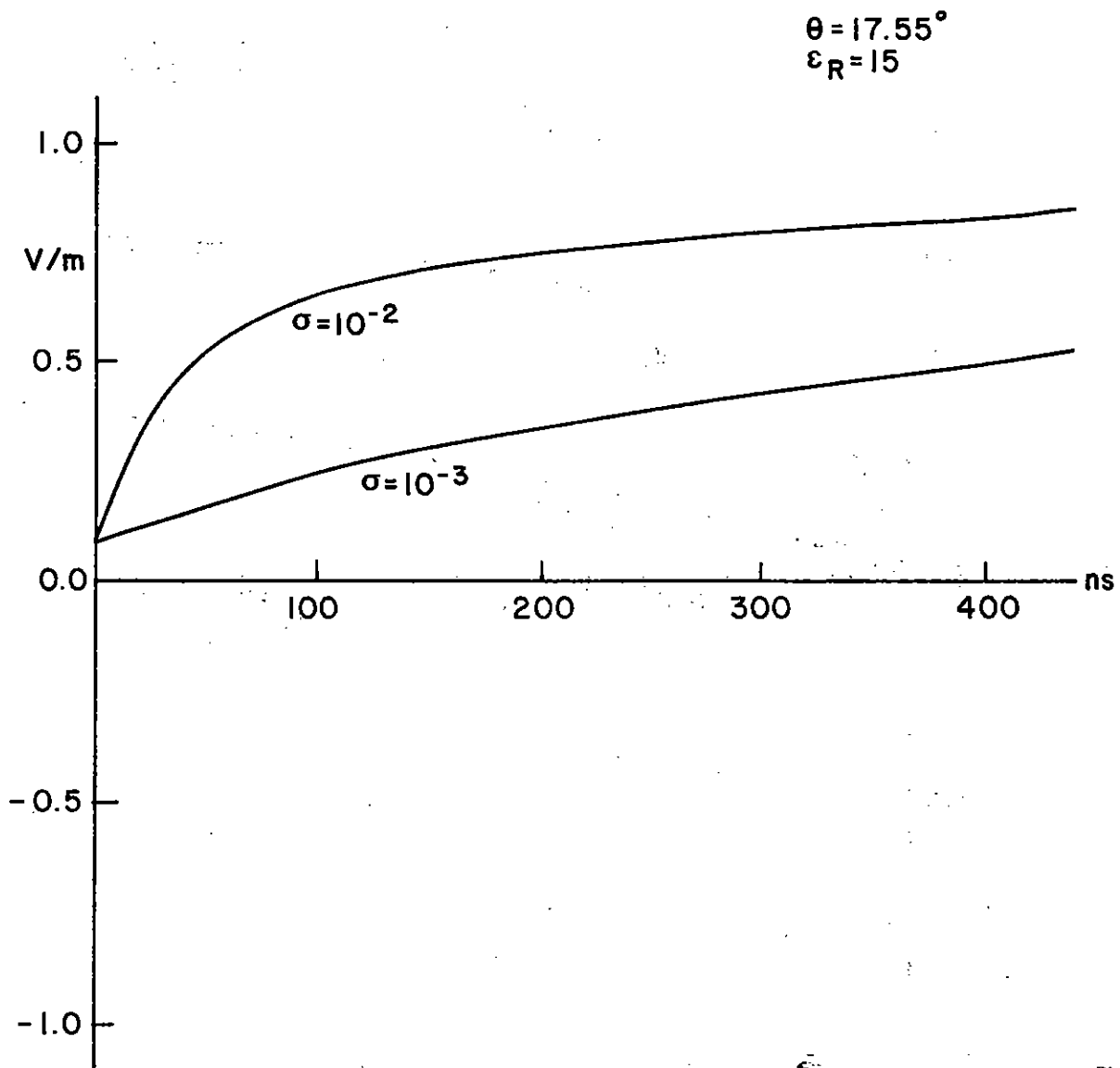


Figure 30. Unit-step response, reflected field:  $\epsilon_R = 15$ ,  $\theta = 17.55^\circ$ .

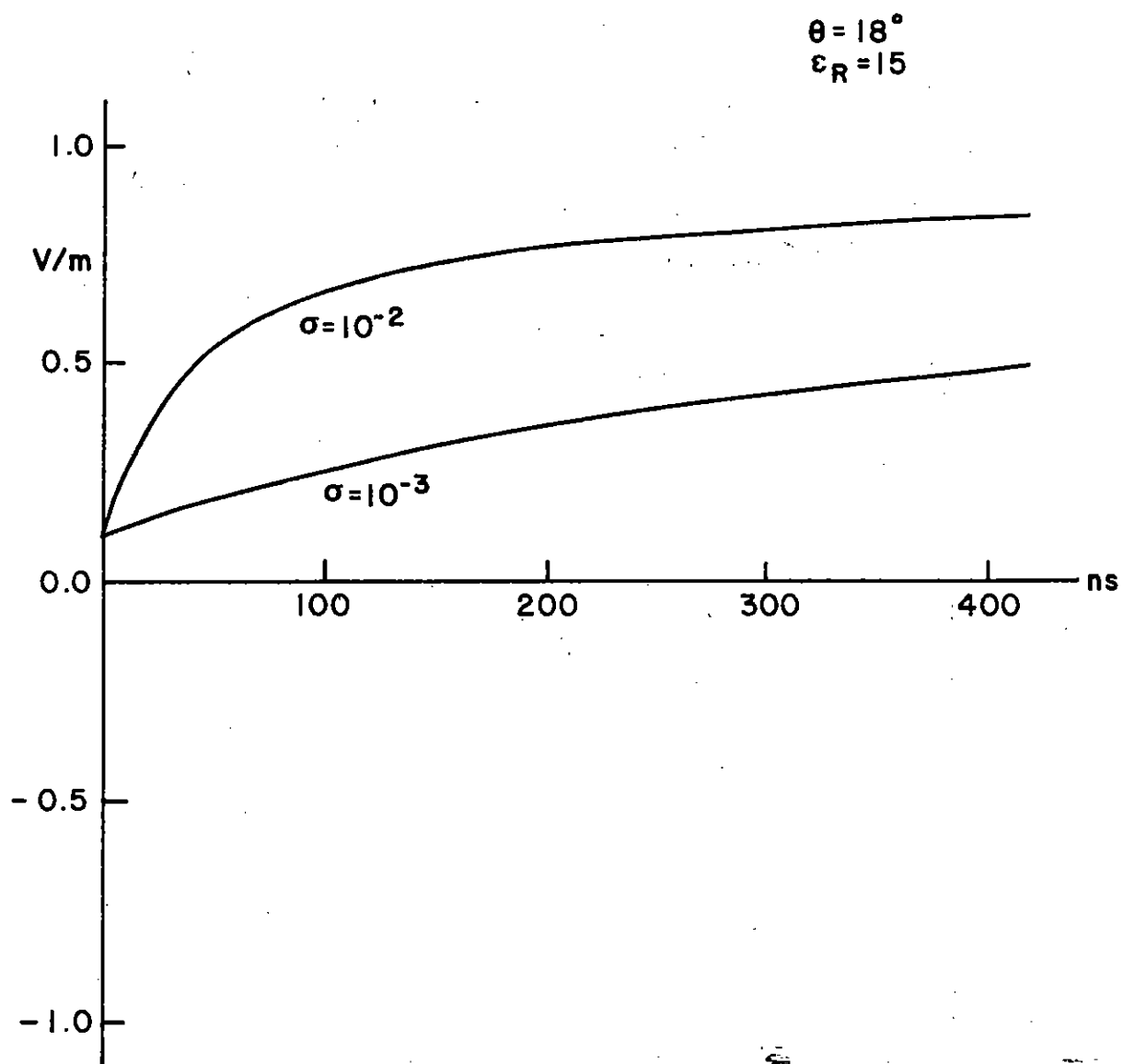


Figure 31. Unit-step response, reflected field:  $\epsilon_R = 15$ ,  $\theta = 18^\circ$ .

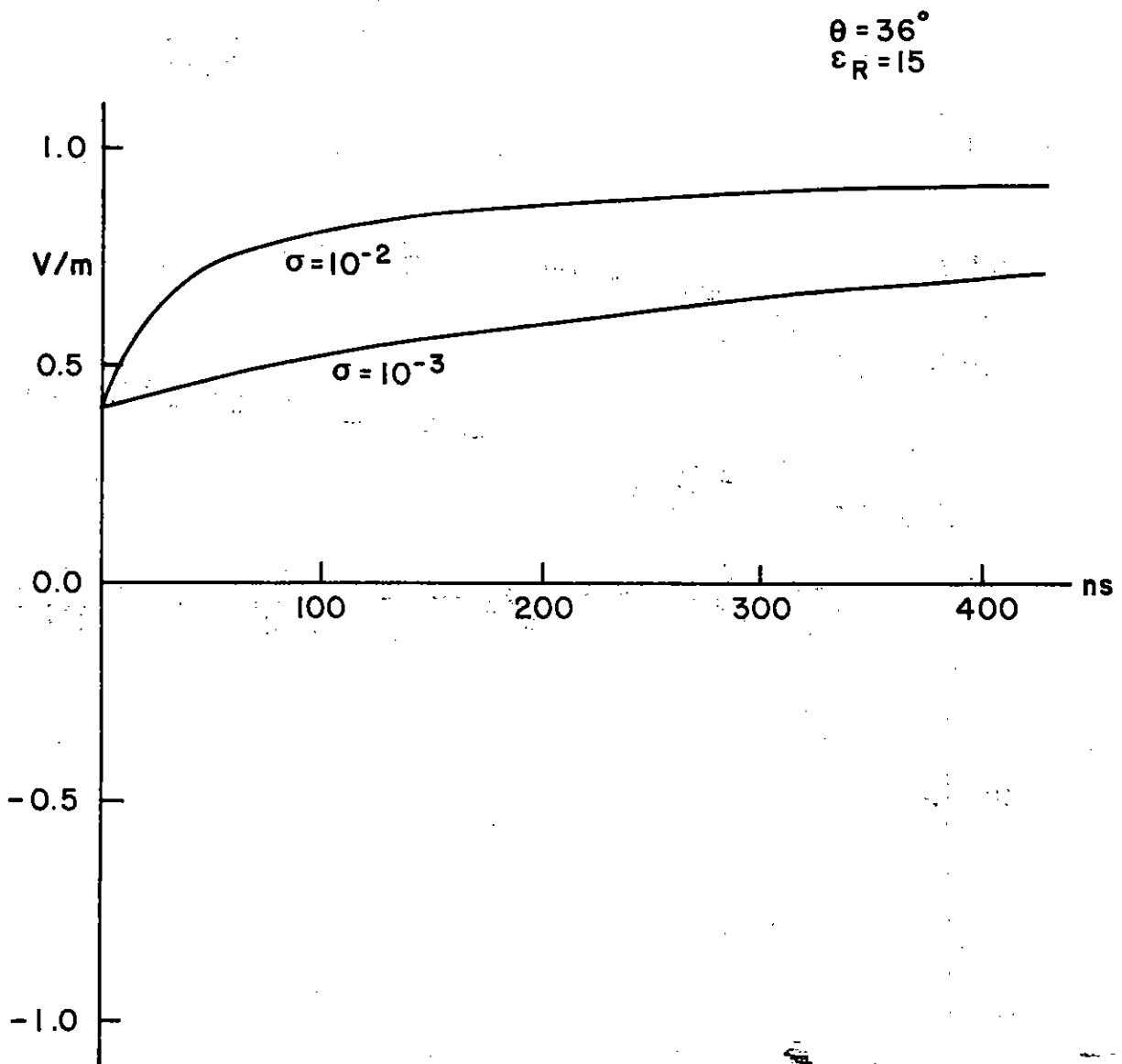


Figure 32. Unit-step response, reflected field:  $\epsilon_R = 15$ ,  $\theta = 36^\circ$ .



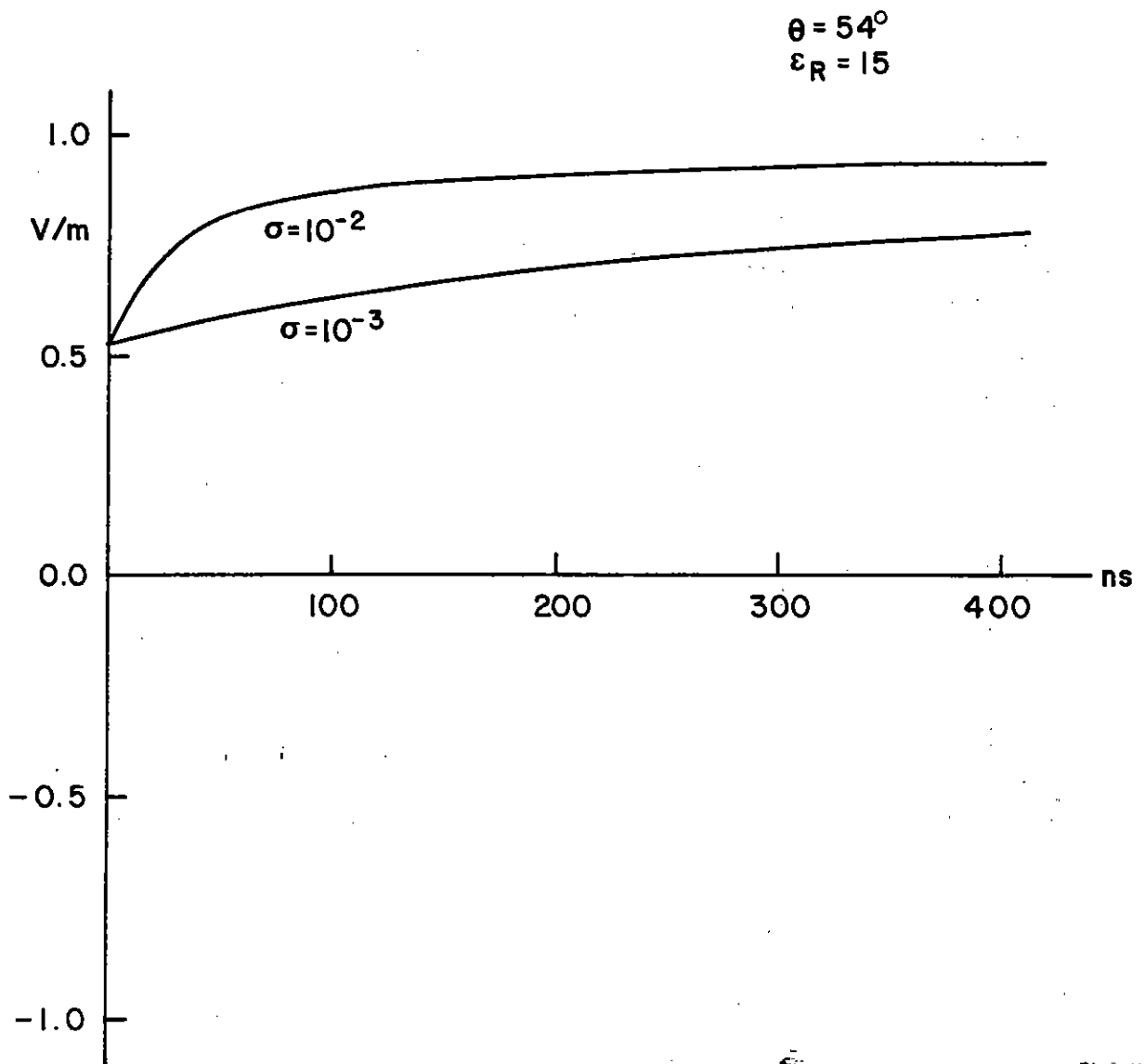


Figure 33. Unit-step response, reflected field:  $\epsilon_R = 15$ ,  $\theta = 54^\circ$ .

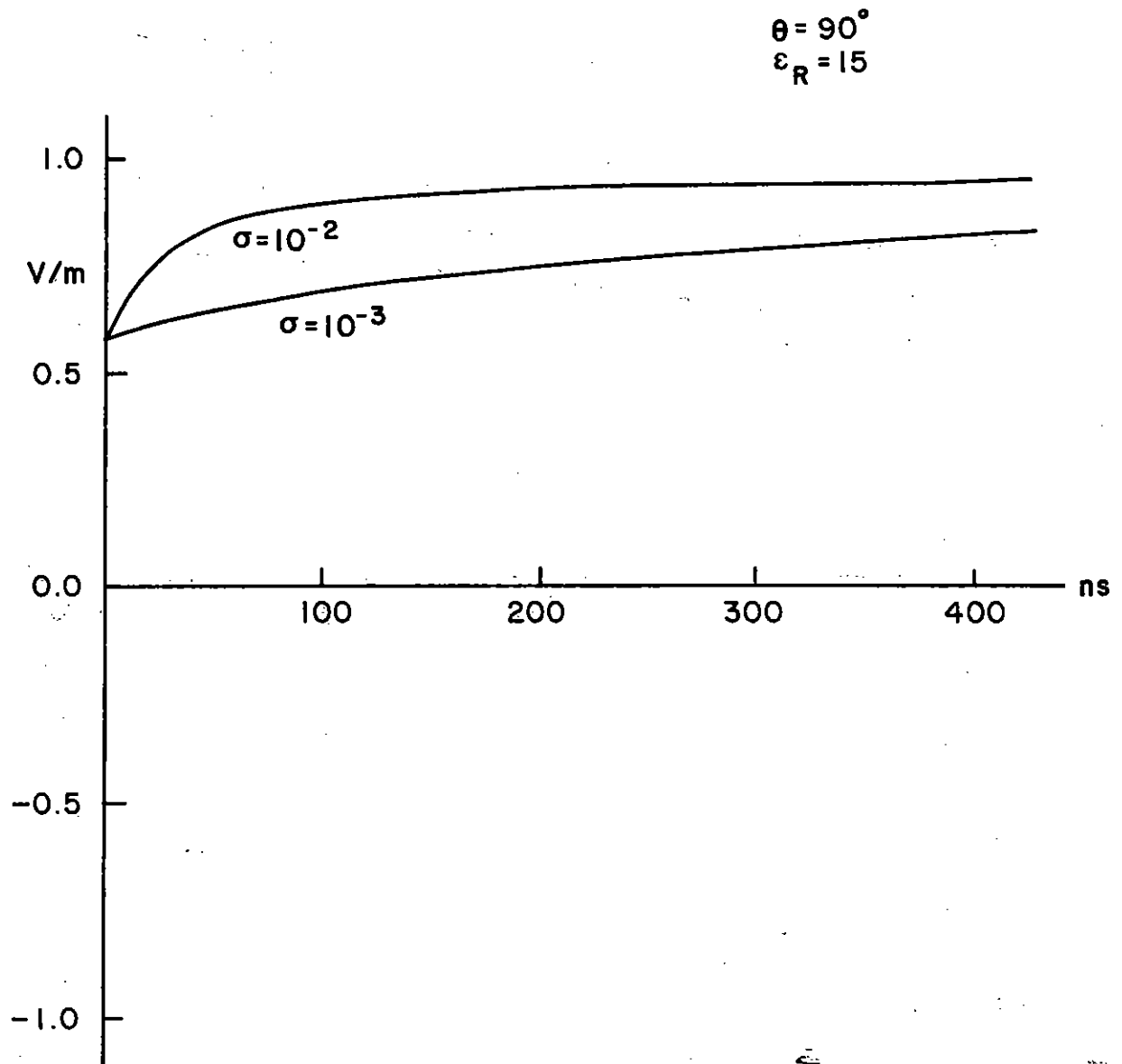


Figure 34. Unit-step response, reflected field:  $\epsilon_R = 15$ ,  $\theta = 90^\circ$ .

#### IV. CONCLUDING REMARKS

The results of this work indicate that for angles greater than the Brewster angle ( $\theta > \theta_B$ ) the composite wave (for the chosen value of  $h$ ) has a peak value determined only by that of the incident wave, and the response is negligible in 400-500 nanoseconds. The conductivity and permittivity of the earth and the height  $h$  will obviously affect the results. On the other hand, for angles less than the Brewster angle ( $\theta < \theta_B$ ), the peak value of the composite wave may be larger than the incident wave. Generally speaking, this effect will be more pronounced for "poor" earth parameters. These results are important in determining the rise time, fall time, and peak value of the current induced in a long wire located above (and parallel to) the earth's surface.

## REFERENCES

1. E. C. Jordan and K. G. Balmain, Electromagnetic Waves and Radiating Systems, Prentice-Hall, Inc. (1968), pp. 143 ff.
2. C. E. Baum, "The Reflection of Pulsed Waves from the Surface of a Conducting Dielectric," Theoretical Notes, TN25, AFWL, Kirtland AFB, NM, February 1967.